

AD-A088 848

NAVAL OCEAN SYSTEMS CENTER SAN DIEGO CA  
GEOMAGNETIC ACTIVITY AND THE EQUATORIAL SCINTILLATION OF SATELL--ETC(U)  
MAY 80 M R PAULSON  
NOSC/TR-554

F/6 17/2.1

NL

UNCLASSIFIED

1 OF 1  
AD-A08864R

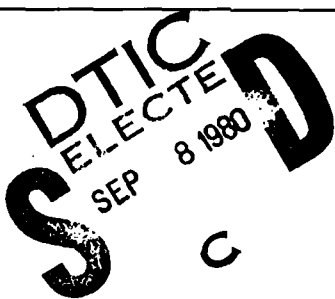
NOSC

END  
DATA INDEXED  
10-80  
DTIC

LEVEL  
*(12)*

# NOSC

NOSC TR 554



C Technical Report 554

NOSC TR 554

AD A 088848

## GEOMAGNETIC ACTIVITY AND THE EQUATORIAL SCINTILLATION OF SATELLITE SIGNALS

M. R. Paulson

19 May 1980

Prepared for  
Office of Naval Research (Code 465)  
Arlington, VA 22217

Approved for public release; distribution unlimited

NAVAL OCEAN SYSTEMS CENTER  
SAN DIEGO, CALIFORNIA 92152

DDC FILE QOPYL

80 9 4 029



NAVAL OCEAN SYSTEMS CENTER, SAN DIEGO, CA 92152

---

A N A C T I V I T Y O F T H E N A V A L M A T E R I A L C O M M A N D

---

**SL GUILLE, CAPT, USN**

Commander

**HL BLOOD**

Technical Director

**ADMINISTRATIVE INFORMATION**

The work reported here was performed under element 61153N, project RR03208, task area RR0320801, and work unit 532-MP41 by members of the EM Propagation Division with assistance from personnel of the Naval Communications Area Master Station, Guam. Extensive assistance by personnel at the NASA tracking station, Dandan, Guam, was also received. This report covers work from March 1978 to December 1979 and was approved for publication 5 May 1980.

Released by  
Dr. J.H. Richter, Head  
EM Propagation Division

Under authority of  
J.D. Hightower, Head  
Environmental Sciences Department

**ACKNOWLEDGEMENTS**

Uhf and L-band satellite signal measurements used in this report were made by personnel at the NASA Tracking Station in Dandan, Guam, under the direction of John Cornwell. Some additional uhf signal measurements used were made by personnel at the Naval Communication Area Master Station (NAVCAMS), Guam, under the direction of RM-1 R.D. Smith.

UNCLASSIFIED

SECURITY CLASSIFICATION OF THIS PAGE (When Data Entered)

(14) NOSC/TR-554

REPORT DOCUMENTATION PAGE		READ INSTRUCTIONS BEFORE COMPLETING FORM
1. REPORT NUMBER NOSC Technical Report 554 (TR 554)	2. GOVT ACCESSION NO.	3. RECIPIENT'S CATALOG NUMBER
4. TITLE (and Subtitle) GEOMAGNETIC ACTIVITY AND THE EQUATORIAL SCINTILLATION OF SATELLITE SIGNALS		5. TYPE OF REPORT & PERIOD COVERED Final Report, March 1978 - December 1979
6. AUTHOR(s) M.R. Paulson		6. PERFORMING ORG. REPORT NUMBER
7. CONTRACT OR GRANT NUMBER(s)		10. PROGRAM ELEMENT, PROJECT, TASK AREA & WORK UNIT NUMBERS 61153N RR03208 RR0320801 532-MP41
8. PERFORMING ORGANIZATION NAME AND ADDRESS Naval Ocean Systems Center San Diego, CA 92152		11. REPORT DATE 19 May 1980
12. CONTROLLING OFFICE NAME AND ADDRESS		13. NUMBER OF PAGES 62
14. MONITORING AGENCY NAME & ADDRESS (if different from Controlling Office)		15. SECURITY CLASS. (of this report) UNCLASSIFIED
16. DISTRIBUTION STATEMENT (of this Report) Approved for public release; distribution unlimited.		15a. DECLASSIFICATION/DOWNGRADING SCHEDULE
17. DISTRIBUTION STATEMENT (of the abstract entered in Block 20, if different from Report)		
18. SUPPLEMENTARY NOTES		
19. KEY WORDS (Continue on reverse side if necessary and identify by block number) Geomagnetism Equatorial scintillation Kp indices Satellites Ionosphere scintillation		
20. ABSTRACT (Continue on reverse side if necessary and identify by block number) Occurrence and intensity of equatorial scintillation have been correlated with daily summed geomagnetic 3-hour Kp indices, through scintillation data from satellites at two elevation angles for UHF and L-band. They also have been correlated with the individual 3-hour Kp indices and the correlations have been shown as a function of the time of day that the magnetic activity occurred. Correlation values as large as -0.91 and +0.56 were observed. A theory of how geomagnetic activity and equatorial scintillation may be connected is proposed.		

## OBJECTIVE

Investigate the relationship between geomagnetic activity and the equatorial scintillation of satellite signals and, if some relationship is found, try to determine how the two are related.

## RESULTS

Correlations between scintillation activity and geomagnetic activity ranged from -0.91 to +0.56. When correlations between nightly scintillation activity and individual 3-hour K<sub>p</sub> indices showed a maximum for a particular time of day, this maximum usually occurred around 1300-1600 LST for the negative maxima and 0200-0700 LST for the positive ones.

It is proposed that the ionized solar radiation, which causes geomagnetic activity, is affecting the occurrence and intensity of equatorial scintillation by heating the thermosphere and thus increasing or decreasing the zonal winds. The increase or decrease depends on the time, with respect to the equatorial site, that the radiations reach the earth.

## RECOMMENDATIONS

The possible connection between ionized solar radiation and equatorial scintillation needs further investigation. In particular, the part that zonal and meridional winds may play in connecting the two, as well as connecting other phenomena that apparently contribute to the occurrence and intensity of scintillation, needs to be investigated.

Accession For	
NTIS GRA&I	
DDC TAB	
Unannounced	
Justification	
By _____	
Distribution /	
Availability Codes	
Dist	Available and/or special
P	

## **CONTENTS**

<b>INTRODUCTION ... page</b>	<b>5</b>
<b>OBJECTIVE ...</b>	<b>5</b>
<b>BACKGROUND ...</b>	<b>5</b>
<b>DATA ANALYSIS AND RESULTS ...</b>	<b>7</b>
<b>DISCUSSION ...</b>	<b>46</b>
<b>RESULTS ...</b>	<b>47</b>
<b>RECOMMENDATIONS ...</b>	<b>48</b>
<b>REFERENCES ...</b>	<b>49</b>
<b>APPENDIX ...</b>	<b>51</b>

## **ILLUSTRATIONS**

- 1 Cross correlations between total hours per night that scintillation fading exceeded 6 dB and the daily summed 3-hour K<sub>p</sub> indices, using 30-day data samples ... page 8
- 2 Cross correlations between nightly sums of standard deviation divided by the mean for 15-minute time intervals and the daily summed 3-hour K<sub>p</sub> indices, using 30-day data samples ... 9
- 3 Cross correlations between total hours per night that scintillation fading exceeded 6 dB and the 3-hour K<sub>p</sub> indices plotted as a function of the time of the K<sub>p</sub> measurement, using 30-day data samples for F2 ... 11
- 4 The same as figure 3, but for F3, the Pacific Ocean satellite ... 15
- 5 Cross correlations between nightly sums of standard deviation divided by the mean and the 3-hour K<sub>p</sub> indices plotted as a function of the time of the K<sub>p</sub> measurement, using 30-day data samples for F2 ... 19
- 6 The same as figure 5, but for F3 ... 22
- 7 The same as figure 5, but for the L-band signals on F2 ... 25
- 8 Cross correlations between sums of standard deviation divided by the mean prior to local midnight and the 3-hour K<sub>p</sub> indices plotted as a function of the time of the K<sub>p</sub> measurement, using 30-day data samples for F3 ... 28
- 9 The same as figure 8, but using sums of standard deviation divided by the mean between local midnight and 0300 ... 31
- 10 Cross correlations between total hours per night prior to 0200 local time that scintillation fading exceeded 6 dB and the 3-hour K<sub>p</sub> indices plotted as a function of the time of the K<sub>p</sub> measurement, using 30-day data samples for F3 ... 34

*PRECEDING PAGE BLANK-NOT FILMED*

#### **ILLUSTRATIONS (Continued)**

- 11 The same as figure 10, but using total hours per night after 0200 local time that scintillation fading exceeded 6 dB ... 38
- 12 Cross correlations between total hours per night that scintillation fading exceeded 6 dB and the 3-hour K<sub>p</sub> indices plotted as a function of the time of the K<sub>p</sub> measurement, using 15-day data samples for F3 ... 42

## INTRODUCTION

During their investigations of the equatorial scintillation of satellite signals, several workers have looked for a possible connection between scintillation activity and geomagnetic activity.

Because of electric currents flowing above the earth's surface, the magnetic field at any point on the surface varies diurnally, seasonally, and with solar activity (ref 1). On days when the magnetic variations are smooth and regular, they proceed mainly according to local solar time; however, a small part of the variation is controlled by the moon. During a magnetic storm, additional currents circulate in the ionosphere and are strong in the high latitudes. These strong additional currents lead to fluctuations in the direction and intensity of the magnetic field as measured at the earth's surface. The currents are believed to be one of many effects caused by the impact of a solar stream, or cloud, of ionized gas on the earth's magnetic field.

The degree of magnetic disturbance during each Greenwich day is indicated by a variety of indices. One of the indices is K<sub>p</sub>. Called the planetary 3-hour index, K<sub>p</sub> ranges in value from 0 to 9 in steps of 1/3 to provide 28 intervals. K<sub>p</sub> values are determined for each 3-hour interval during the day.

Additional information on geomagnetic activity and indices is available in reference 1.

Since March 1978, personnel at the Naval Communications Area Master Station, Guam, have been recording the amplitude of uhf signals from two MARISAT/GAPFILLER satellites, one positioned over the Indian Ocean, F2, and one over the Pacific Ocean, F3. F2 has an elevation angle from Guam of about 10 degrees and F3 about 50 degrees. In addition, personnel at the NASA Tracking Station in Dandan, Guam, recorded both uhf and L-band signals from these two satellites for the period from late February through December 1979. An extensive analysis of these data was reported in reference 2. This report will be limited to an investigation of the relationship between equatorial scintillation observed in the above data and geomagnetic activity.

## OBJECTIVE

The objective of this work is to look for a relationship between geomagnetic activity and equatorial scintillation activity, using the data recorded at Guam; and, if some relationship is found, to try to determine how the two are related.

## BACKGROUND

Koster (ref 3) says that the usual way of comparing scintillation activity and geomagnetic activity is to calculate the correlation between daily sums of the 3-hour K<sub>p</sub> and the scintillation indices. The results, he says, are far from clear or consistent. A zero or low correlation can mean that there is no relationship between the variables, or that the relationship is nonlinear. He says that the latter is true in this case.

1. National Bureau of Standards Monograph 80, Ionospheric Radio Propagation, by K. Davies, U.S. Government Printing Office, 1965.
2. Naval Ocean Systems Center TR 543, Equatorial Scintillation of Satellite Signals at UHF and L-Band for Two Different Elevation Angles, by M.R. Paulson, in progress.
3. Koster, J.P., Equatorial Scintillation, Planetary Space Science, v 20, pp 1999 - 2014, 1972.

Koster studied scintillation activity for various levels of magnetic activity. The study was limited to two daily intervals, 0000 - 0430 and 1930 - 2400 local time. The daily sum of K<sub>p</sub> was taken as a measure of magnetic activity, and days were grouped according to whether this sum fell in the range 0 - 3, 3 - 6, etc. Six normalized monthly means of scintillation index were plotted for each range. He found the results for premidnight and for postmidnight virtually identical. On days when the sum of K<sub>p</sub> was less than 30, there was no obvious dependence of scintillation on K<sub>p</sub>. On days when this sum was equal to or greater than 30, the scintillation intensity was usually, but not always, reduced. This was true for both pre- and postmidnight periods.

Koster concludes that the relationship between scintillation intensity and magnetic activity at Legon, Ghana, is extremely nonlinear, so that calculation of a correlation coefficient between the two is not very useful. Furthermore, nighttime scintillation is frequently absent at Legon during times of severe magnetic disturbances.

Bandyopadhyay and Aarons (ref 4) investigated scintillation by means of data recorded at Huancayo, Peru, between July 1967 and February 1969. The signals used were transmitted from two geosynchronous satellites at 137 MHz. When they plotted the mean hourly scintillation index for the period from 1900 to 0700 against the sum of the 3-hour K<sub>p</sub> indices at Huancayo for the same night, they found no trends. When they used hourly means of scintillation indices between 1800 and 0600 LST to determine the occurrence of scintillation intensity greater than 40% during various levels of magnetic activity, they concluded that there was no significant dependence. In particular, they said that during this period of high sunspot number the scintillations were not negatively correlated with K<sub>p</sub>.

Mullen (ref 5) made use of 136-MHz satellite data also recorded at Huancayo, Peru, to investigate the seasonal and magnetic dependence of equatorial scintillation. Over 13,000 hours of amplitude data recorded from January 1968 through the end of 1970 were used. Hourly scintillation indices were calculated for the data; then those which had indices greater than 20% were sorted into pre- and postmidnight periods for four seasonal groups.

Mullen used an hourly Dst magnetic index to study magnetic activity dependence. A Dst less than or equal to -20 was considered an indication of disturbed magnetic conditions. The scintillation data were then sorted into periods for disturbed and undisturbed magnetic activity for each of the pre- and postmidnight periods for each of the seasons. He says that the most obvious effect is the increase in scintillation occurrence during the June solstice during magnetically disturbed periods.

For the premidnight hours during the December solstice, the occurrence of scintillation was higher during quiet periods than during disturbed periods. For the March equinox, Mullen found scintillation much more common during quiet magnetic periods than during disturbed periods. Premidnight scintillation during the September equinox was similar for the quiet and the disturbed periods but, for postmidnight periods, it was significantly higher during disturbed periods.

In view of the varied and complex results uncovered by the above workers, it appeared that an investigation into the relationship between geomagnetic activity and the equatorial scintillation data recorded at Guam should be undertaken. Not only is Guam geographically remote from the African and South American locations where the other studies

4. Bandyopadhyay, P., and J. Aarons, The Equatorial F-Layer Irregularity Extent as Observed from Huancayo, Peru, *Radio Science*, v 5, no 6, pp 931 - 938, June 1970.
5. Mullen, J.P., Sensitivity of Equatorial Scintillation to Magnetic Activity, *Journal of Atmospheric and Terrestrial Physics*, v 35, pp 1187 - 1194, 1973.

were made, but the 257-MHz vhf/uhf and the 1541-MHz L-band frequencies monitored at Guam are considerably higher than the 136-MHz frequency used in the preceding studies.

## DATA ANALYSIS AND RESULTS

Although Koster found the relationship between magnetic activity and scintillation activity to be highly nonlinear, it appeared that the simplest approach, initially, would be to look for a correlation between magnetic activity and the Guam scintillation activity.

Daily total hours of the occurrence of scintillation with fades greater than 6 dB were determined from the uhf records of both the Indian Ocean satellite and the Pacific Ocean satellite, based on the data from 1 January through 31 December 1979. The daily sums of the eight 3-hour  $K_p$  indices, obtained from reference 6, were used as an indicator of magnetic activity. The data were taken in sample periods of about 30 days at 5-day intervals and the calculated correlation value was plotted for the center of the sample period. The results are shown in figure 1.

These correlation curves start out near zero or slightly positive in January and rapidly go negative in February, with values as large as -0.75 for the Indian Ocean satellite and -0.6 for the Pacific Ocean satellite. Values for F3 remain quite negative through the middle of June; then, after going slightly positive in July, they go negative again with values as low as -0.6 in September before going positive in November and December with values around 0.2 to 0.4. Correlation values for F2, the Indian Ocean satellite, start approaching zero in May but stay slightly negative except for one point in July. They again go negative in September before becoming slightly positive in November and December with values on the order of 0.1 to 0.2.

While the two curves are quite similar, there are some differences. These differences may result from the fact that the two satellites had different look angles, with the elevation angle to F2 being about 10 degrees and that for F3 being about 50 degrees. An additional possible reason for the differences is that F2, because of its low look angle, was also susceptible to the occurrence of sporadic-E irregularities.

On the chance that using 6-dB fades as a criterion for scintillation was not a sensitive enough indicator, data from 1 March through December 1979 were digitized and values for standard deviation divided by the mean were calculated for each 15-minute sample. These values were summed for each night for each satellite, and for the L-band as well as the uhf. Correlations between these data and magnetic activity were calculated in a manner identical to that already described. The results are shown in figure 2. The upper two curves are for the uhf for the two satellites and the bottom one is for the L-band for F2. The uhf plots show excellent agreement with corresponding plots in figure 1. Comparing the L-band plot for F2 with the uhf plot for F2 also shows good agreement.

The next step in trying to evaluate the relationship between magnetic activity and equatorial scintillation was to see if the scintillation was more sensitive to magnetic activity occurring during some particular time of day. Again, about 30-day samples were used, this time at 15-day intervals. Daily occurrence of scintillation data was correlated with daily values for each of the eight 3-hour  $K_p$  indices for each of the sample periods. To get a finer structure, additional correlations were calculated with interpolated values of  $K_p$  between the reported points. The results were plotted as correlation value versus the GMT or LST

6. National Oceanic and Atmospheric Administration Environmental Data and Information Service, Solar Geophysical Data, Prompt Reports, Boulder, CO.

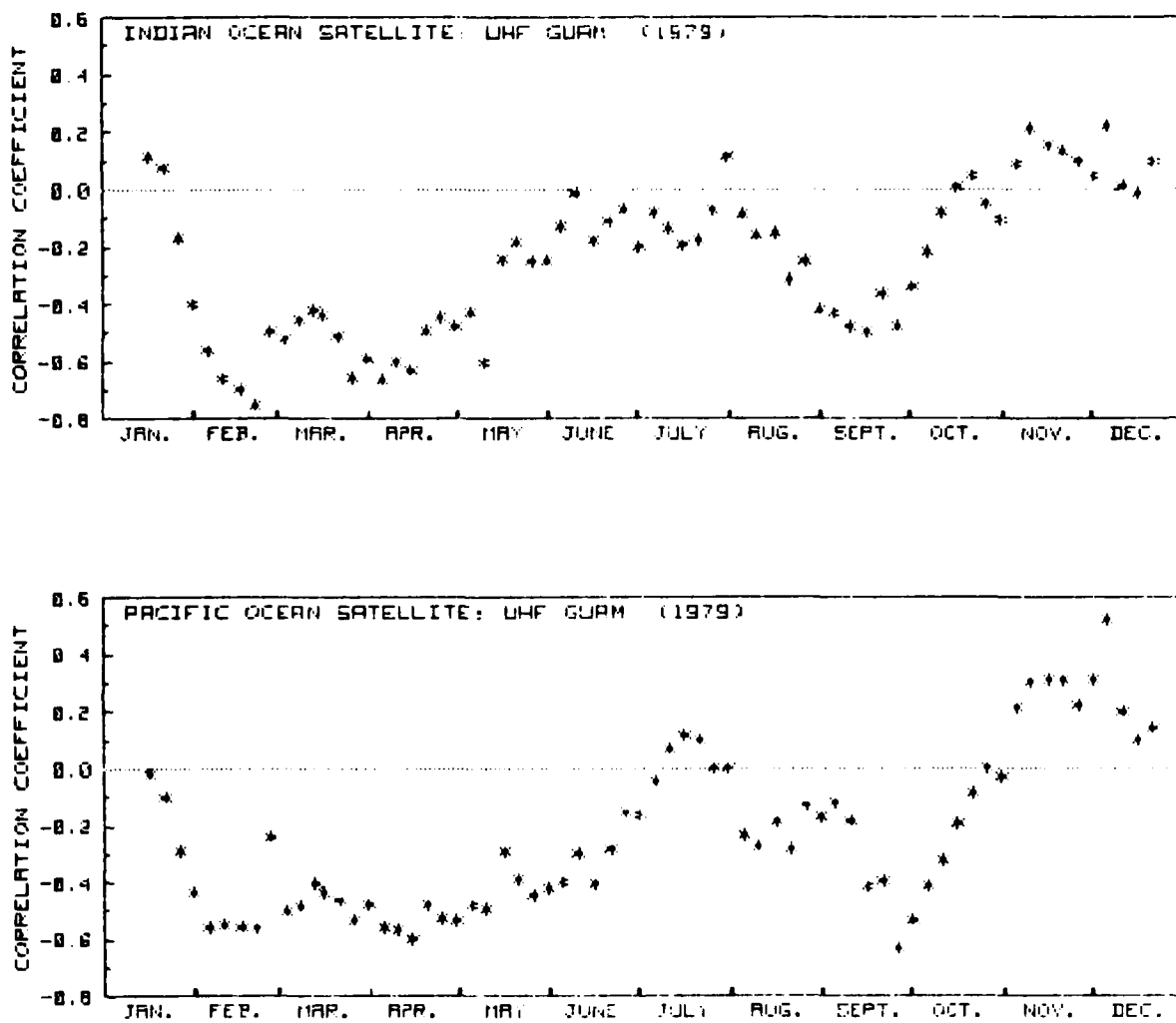


Figure 1. Cross correlations between total hours per night that scintillation fading exceeded 6 dB and the daily summed 3-hour K<sub>p</sub> indices, using 30-day data samples.

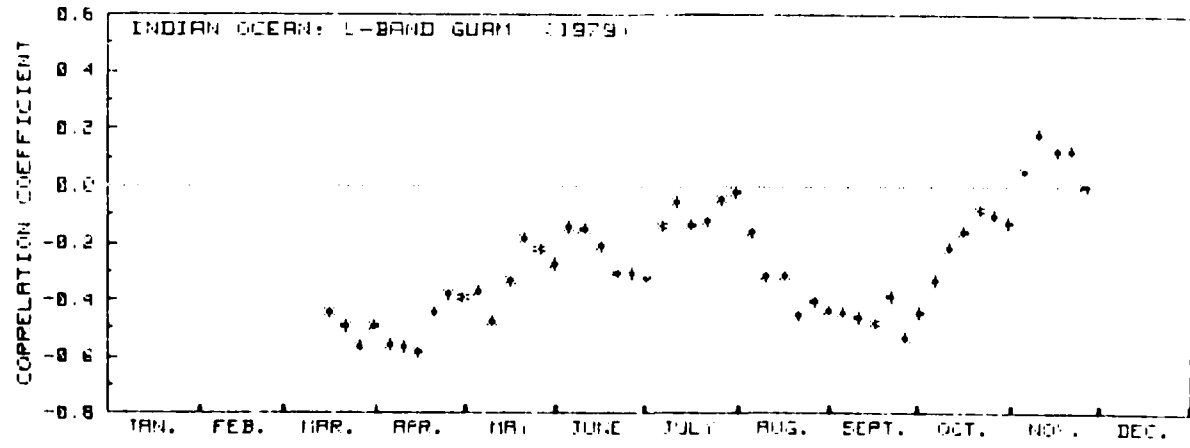
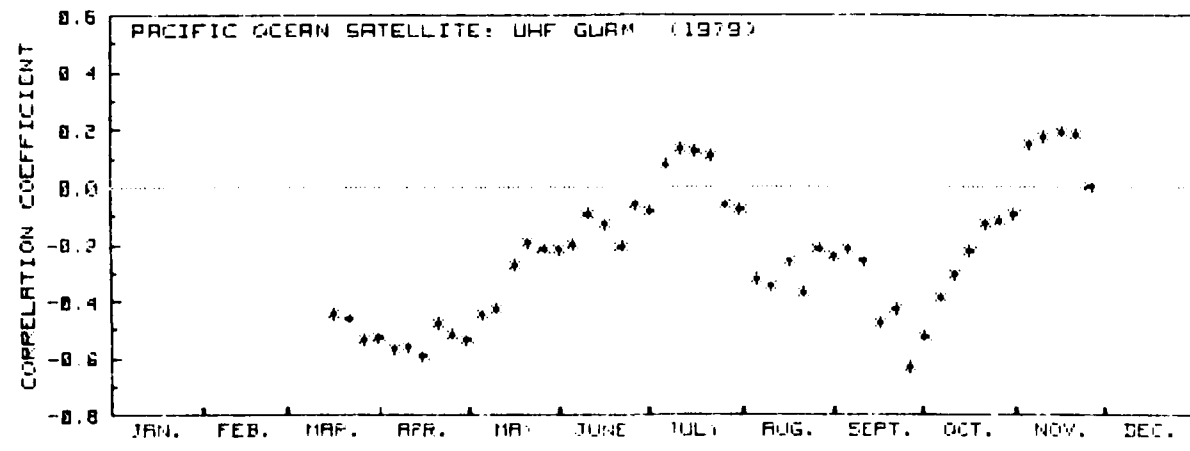
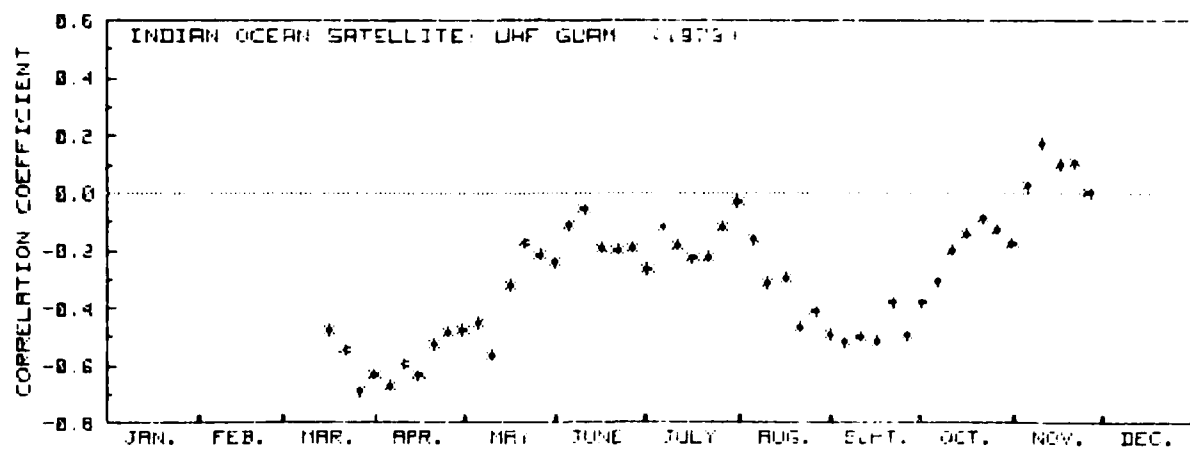


Figure 2. Cross correlations between nightly sums of standard deviation divided by the mean for 15-minute time intervals and the daily summed 3-hour K<sub>p</sub> indices, using 30-day data samples.

when the magnetic activity occurred. These plots were made for each of the data samples and are shown in figures 3 through 7.

Figure 3 comprises the plots for F2 correlations calculated through the use of 6-dB fading data. The plots on the right side are for data overlapping the 2 months. For example, the plot to the right of January is for data from 15 January to 15 February. These plots show results quite similar to those obtained with the total daily K<sub>p</sub> values. In some cases, however, they show a definite maximum negative or positive correlation for a particular time of day. This is especially noticeable for the months of August and September for F2, as shown in figure 3. In figure 4 for F3, it shows up in March and April and again in September. In November, there is a positive maximum for both F2 and F3 but it is most pronounced for F3.

Corresponding plots of correlations that were calculated between standard deviation divided by the mean and daily magnetic activity are shown in figures 5 and 6 for the uhf and in figure 7 for the L-band for F2. The results are quite similar to those in figures 3 and 4.

Maximum negative correlations, when they occurred, were around 1300 to 1600 LST, and maximum positive correlations occurred around 0200 to 0700 LST.

Other workers have been looking for differences in magnetic dependence for pre- and postmidnight scintillation activity. To see if any differences might show up in the Guam data, sums of standard deviation divided by the mean were calculated for premidnight and postmidnight for the uhf on the Pacific Ocean satellite, F3. Cross correlations were calculated as before. These are shown in figure 8 for the premidnight data and in figure 9 for the postmidnight data. Corresponding correlations are quite similar, and are also similar to those calculated for the total night. The biggest differences in the pre- and postmidnight correlations appear to occur in the June and July data.

Since there is probably nothing inherently significant about midnight, a 0200 LST dividing time was used to determine what effect it might have. Daily total hours of scintillation with fades greater than 6 dB were determined for time prior to 0200 LST and for time from 0200 LST on. These were then correlated with magnetic activity as before, and are shown in figures 10 and 11.

The correlation plots for the occurrence of scintillation prior to 0200 LST are quite similar to those for the all-night case shown in figure 4. Again, when there is a definite maximum negative correlation, it occurs around 1300 to 1600 LST.

The cross correlation for the after-0200 scintillation show many differences. July and August show positive correlations, as do October through December. August and September show negative correlation for one part of the day and positive correlation for another.

To determine what effect varying the sample size might have on the correlations, the total hours per day that fades exceeded 6 dB were used for the Pacific Ocean satellite uhf in about 15-day samples, and the correlations calculated. The results are plotted in figure 12 and tabulated in table X in appendix A. Maximum negative values are seen for the last 2 weeks of March and the first 2 weeks of April for the time period around 1300 to 1600 LST. The values were -0.79 and -0.70, respectively. Even larger negative correlations are seen for the last 2 weeks in April, but there is no sharp peak in the curve. Another negative peak is seen around 1300 LST for the last 2 weeks in September. This had a value of -0.91. Positive correlations are seen in July and November, with a value of 0.51 during the first 2 weeks of November occurring around 0400 LST.

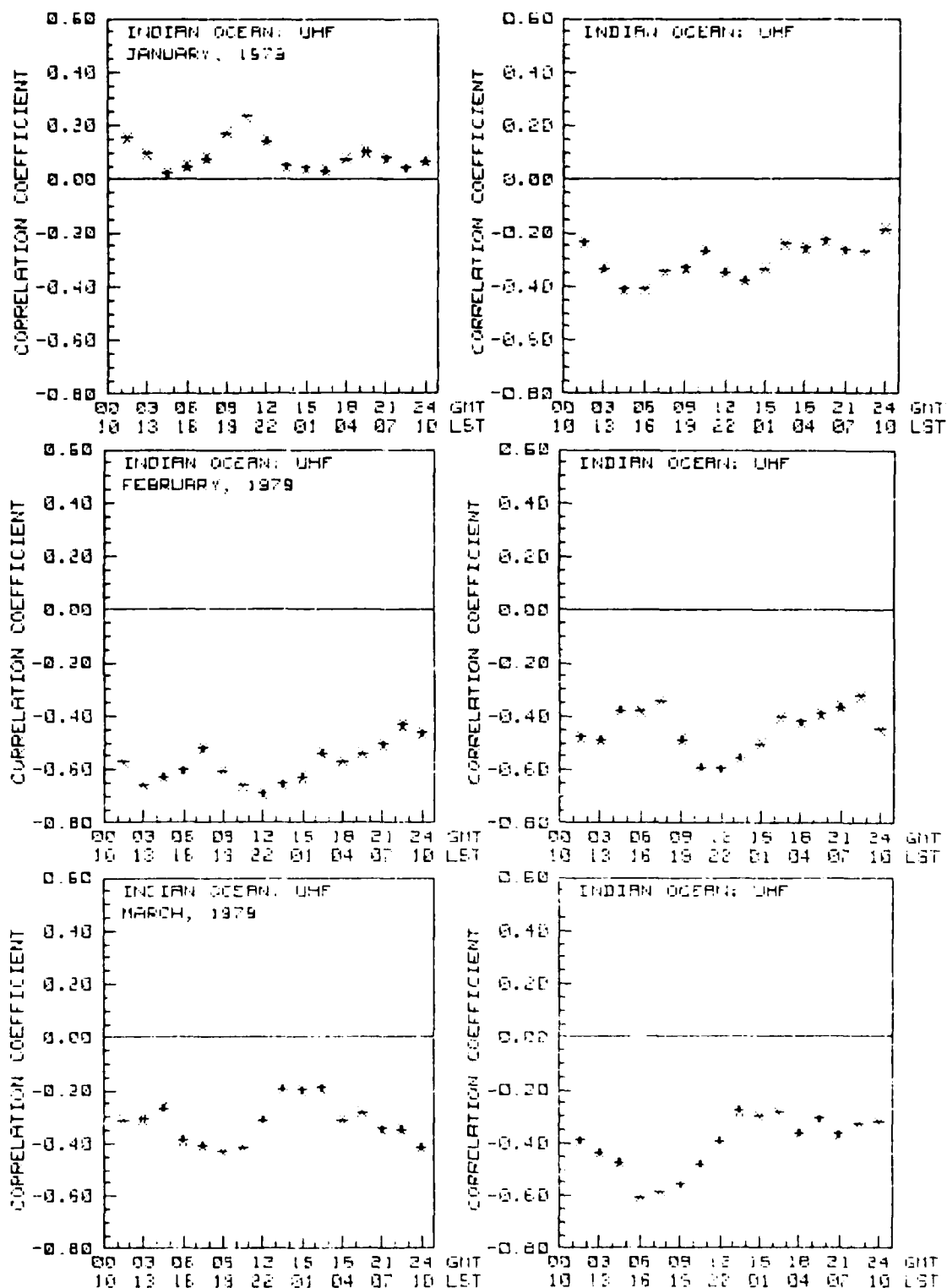


Figure 3. Cross correlations between total hours per night that scintillation fading exceeded 6 dB and the 3-hour K<sub>p</sub> indices plotted as a function of the time of the K<sub>p</sub> measurement, using 30-day data samples for F2.

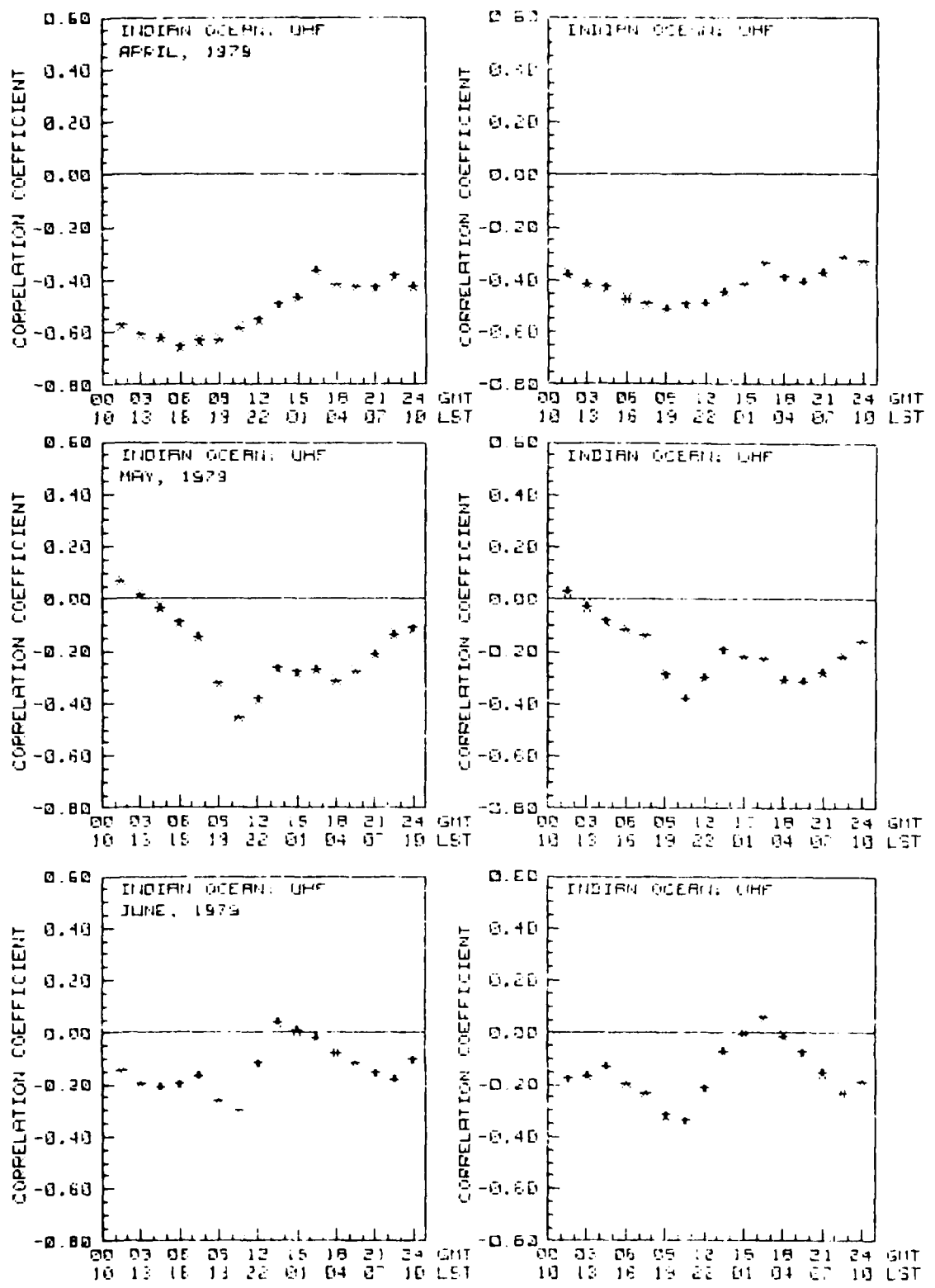


Figure 3. Cross correlations between total hours per night that scintillation fading exceeded 6 dB and the 3-hour K<sub>p</sub> indices plotted as a function of the time of the K<sub>p</sub> measurement, using 30-day data samples for F2. (Continued)

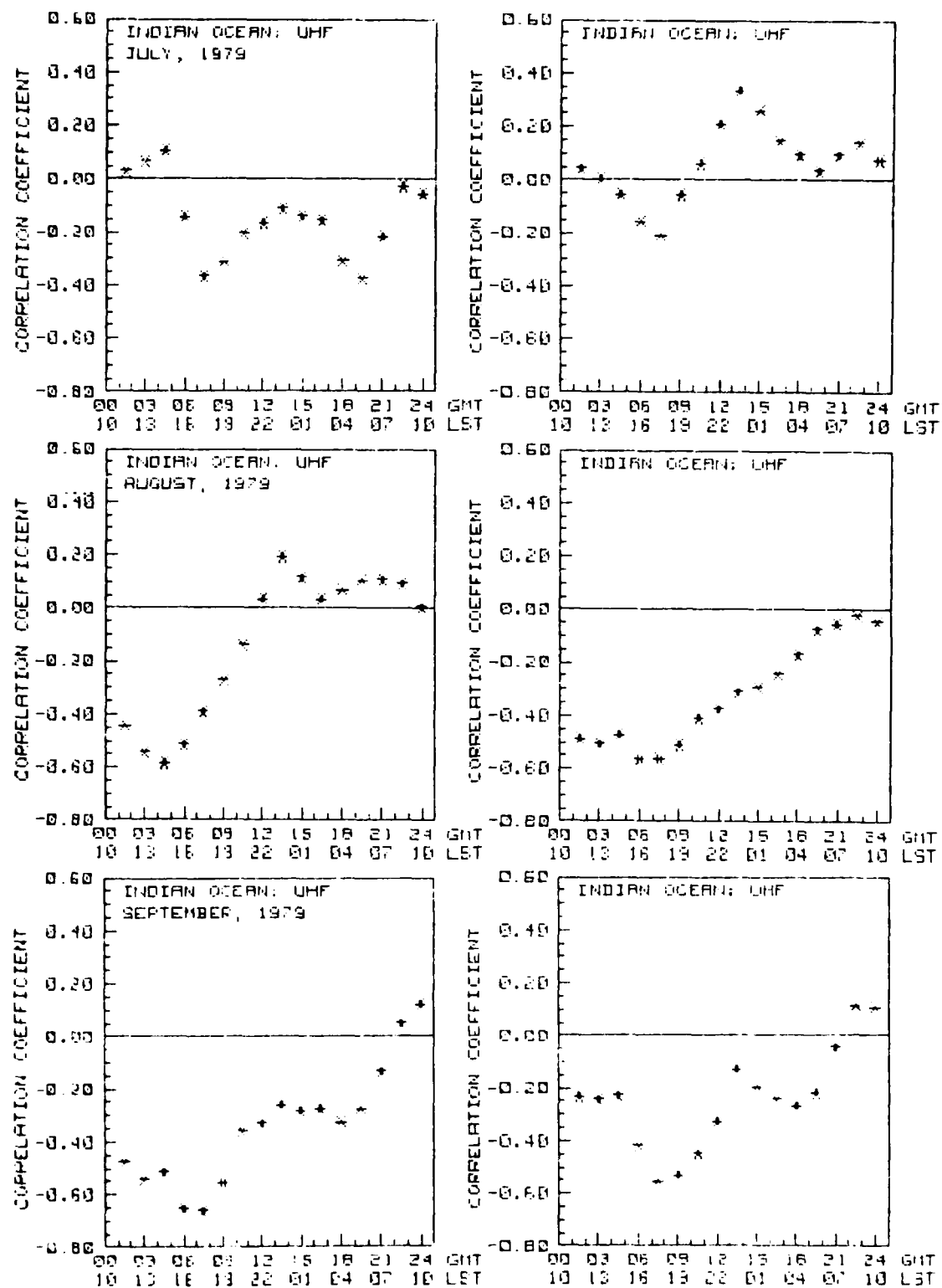


Figure 3. Cross correlations between total hours per night that scintillation fading exceeded 6 dB and the 1-hour  $K_p$  indices plotted as a function of the time of the  $K_p$  measurement, using 30-day data samples for F2. (Continued)

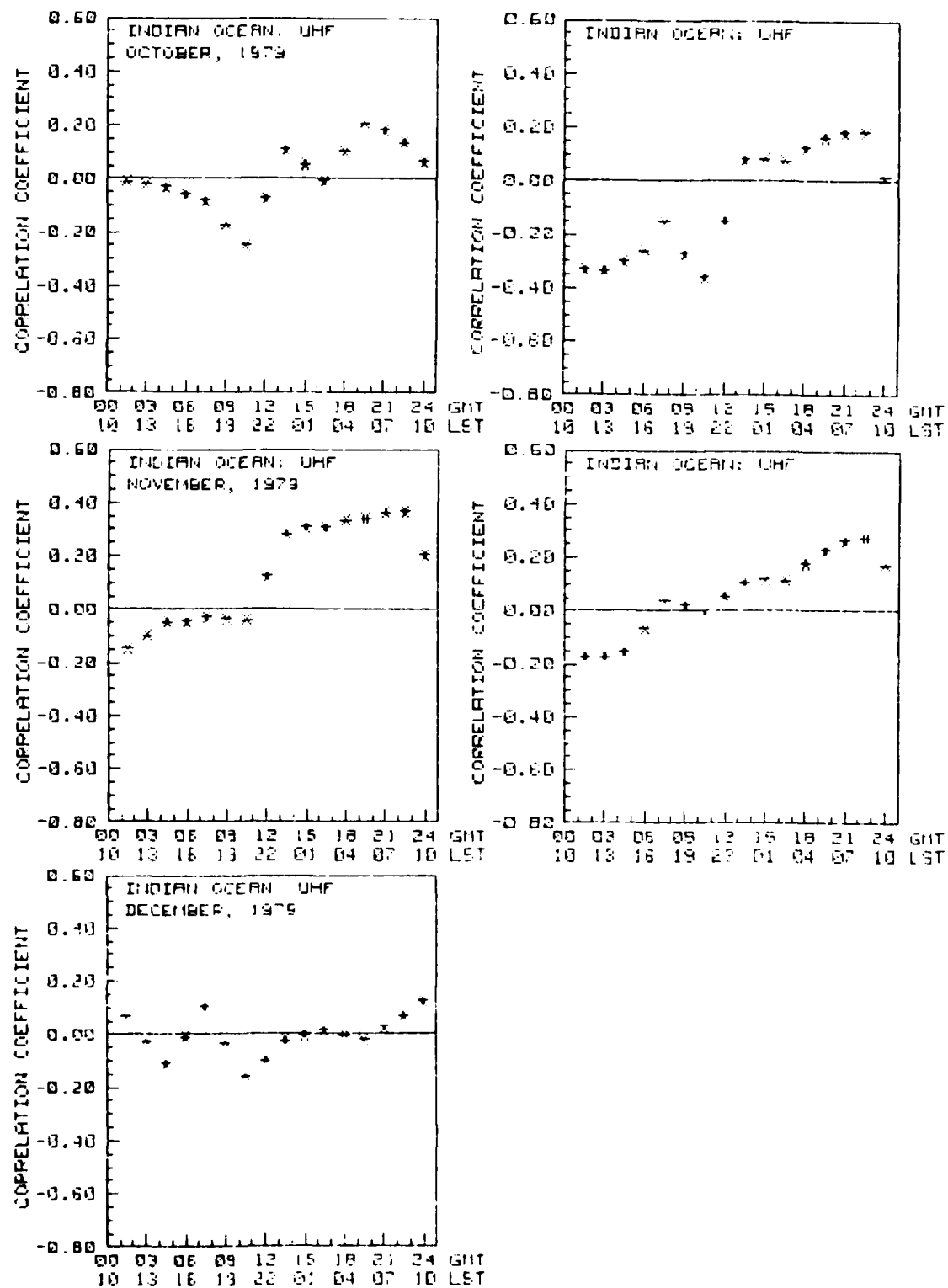


Figure 3. Cross correlations between total hours per night that scintillation fading exceeded 6 dB and the 3-hour K<sub>p</sub> indices plotted as a function of the time of the K<sub>p</sub> measurement, using 30-day data samples for F2. (Continued)

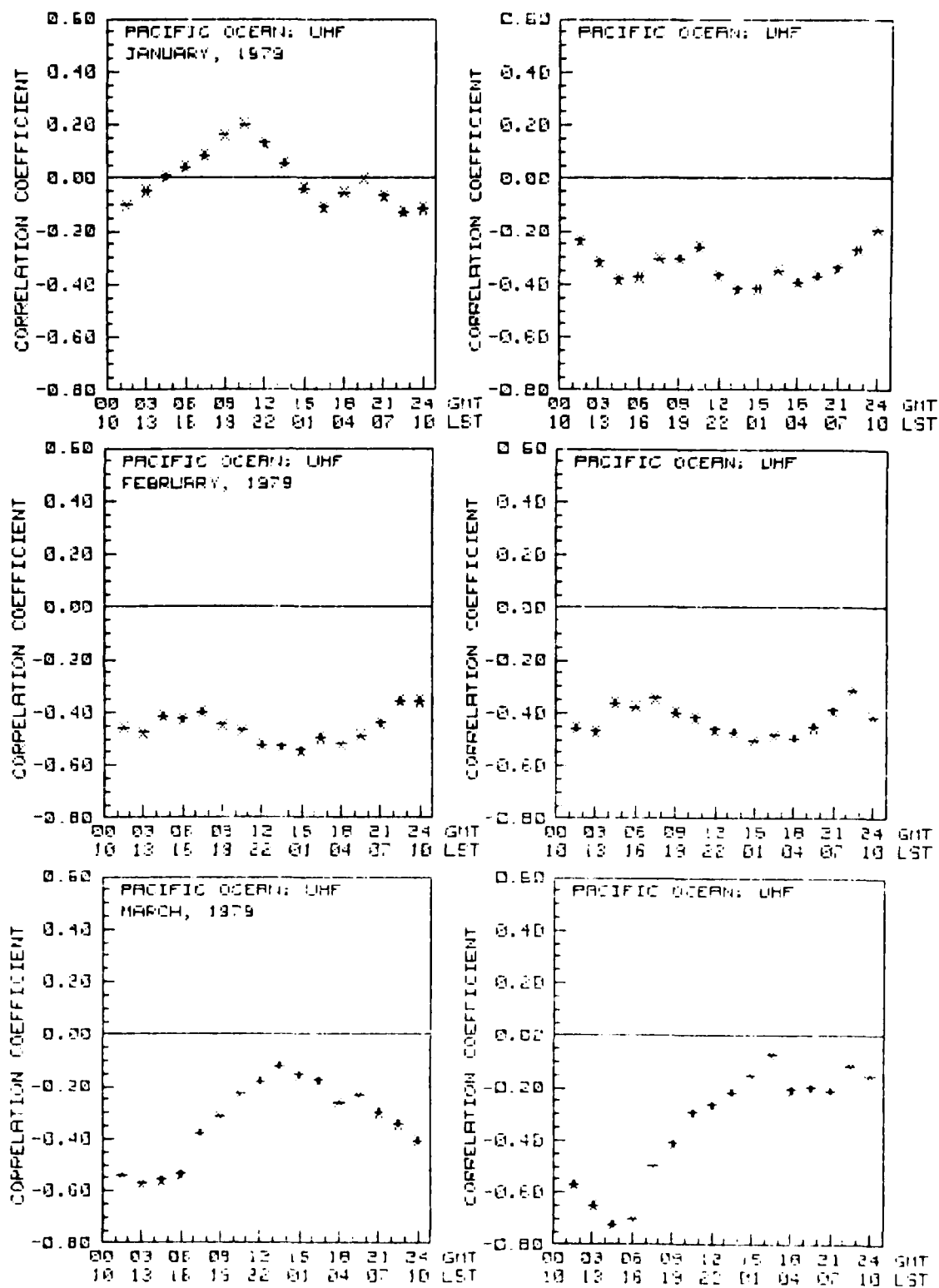


Figure 4. The same as figure 3, but for F3, the Pacific Ocean satellite.

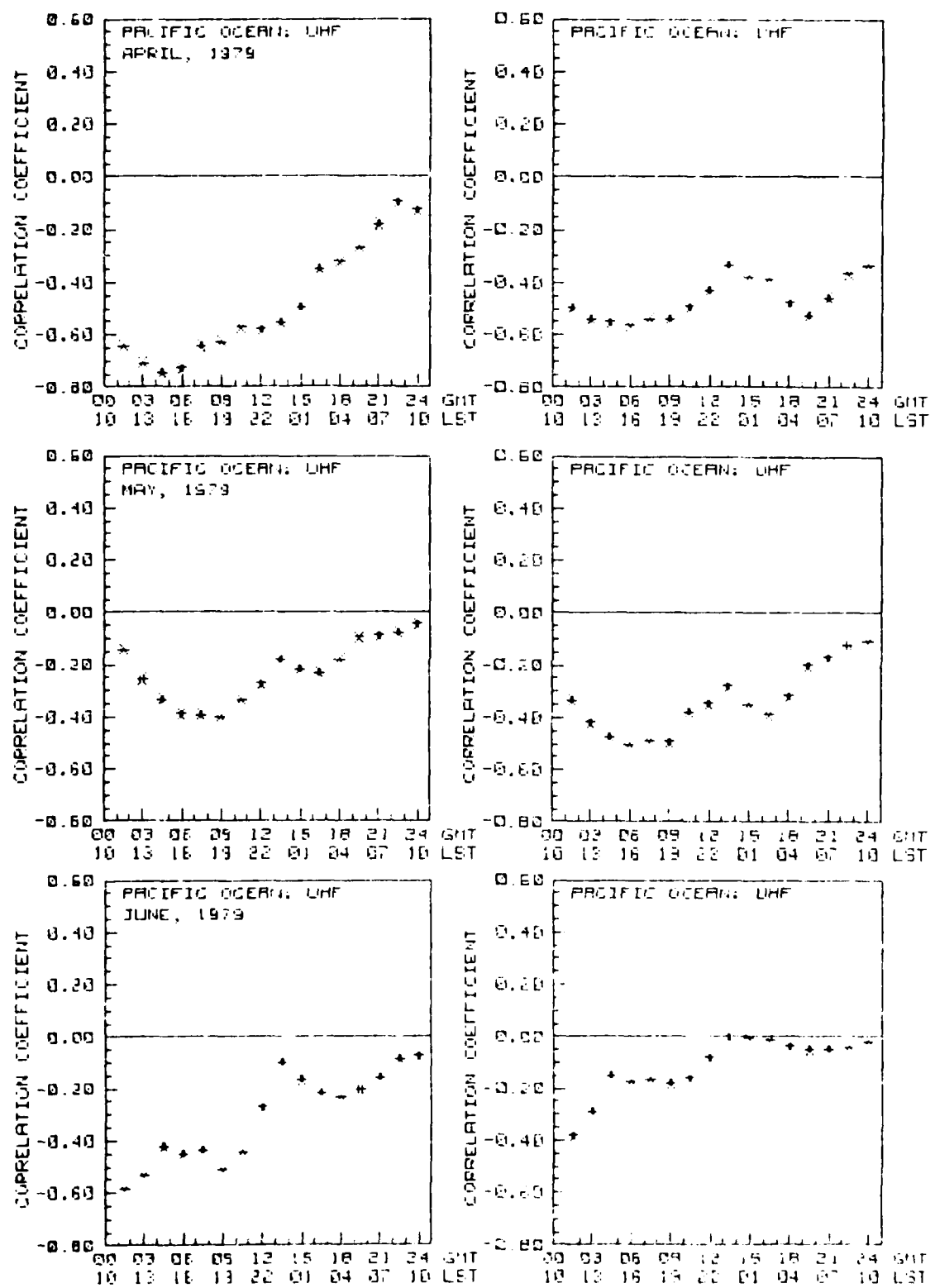


Figure 4. The same as figure 3, but for F3, the Pacific Ocean satellite. (Continued)

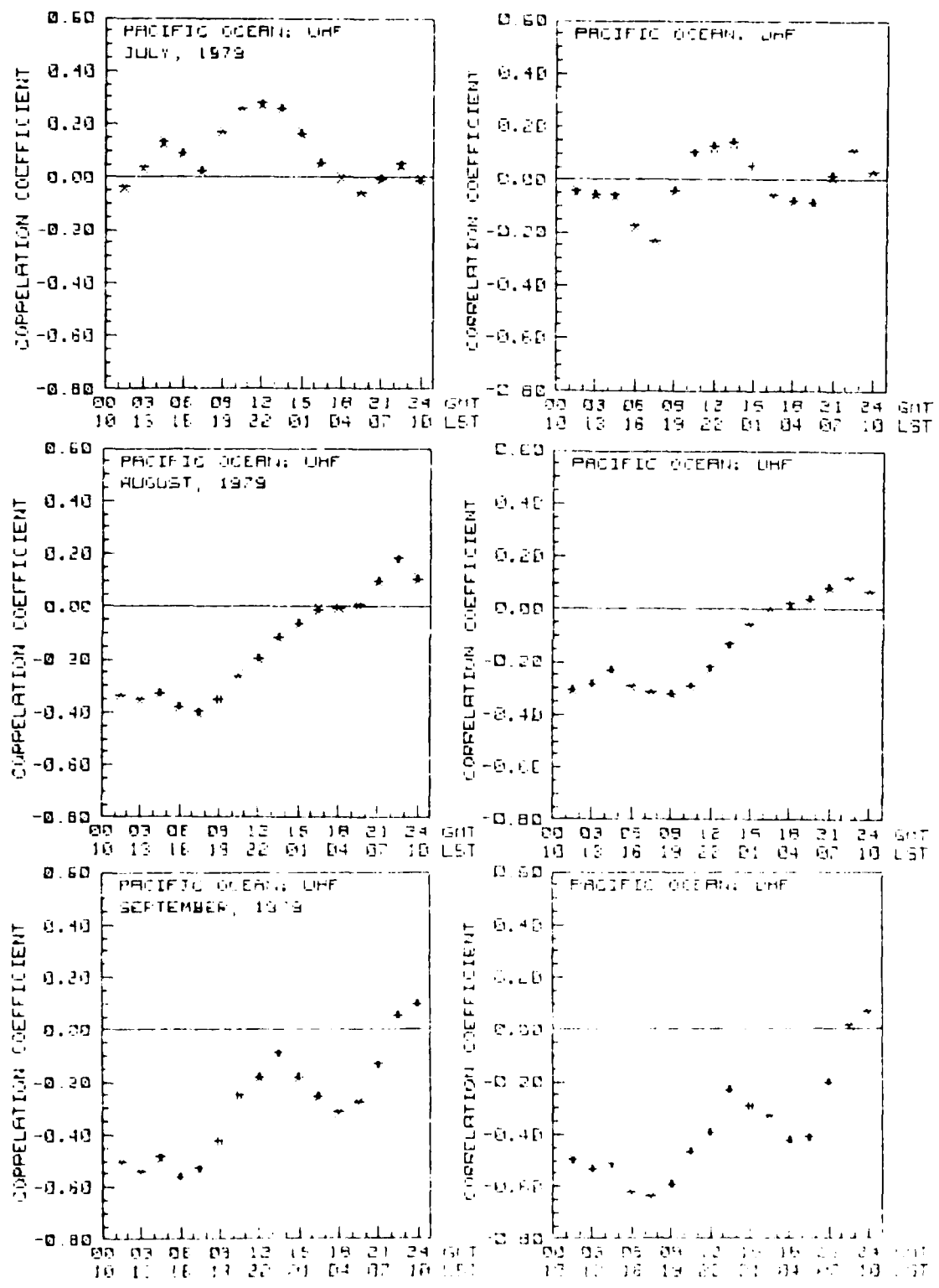


Figure 4. The same as figure 3, but for E3, the Pacific Ocean satellite. (Continued)

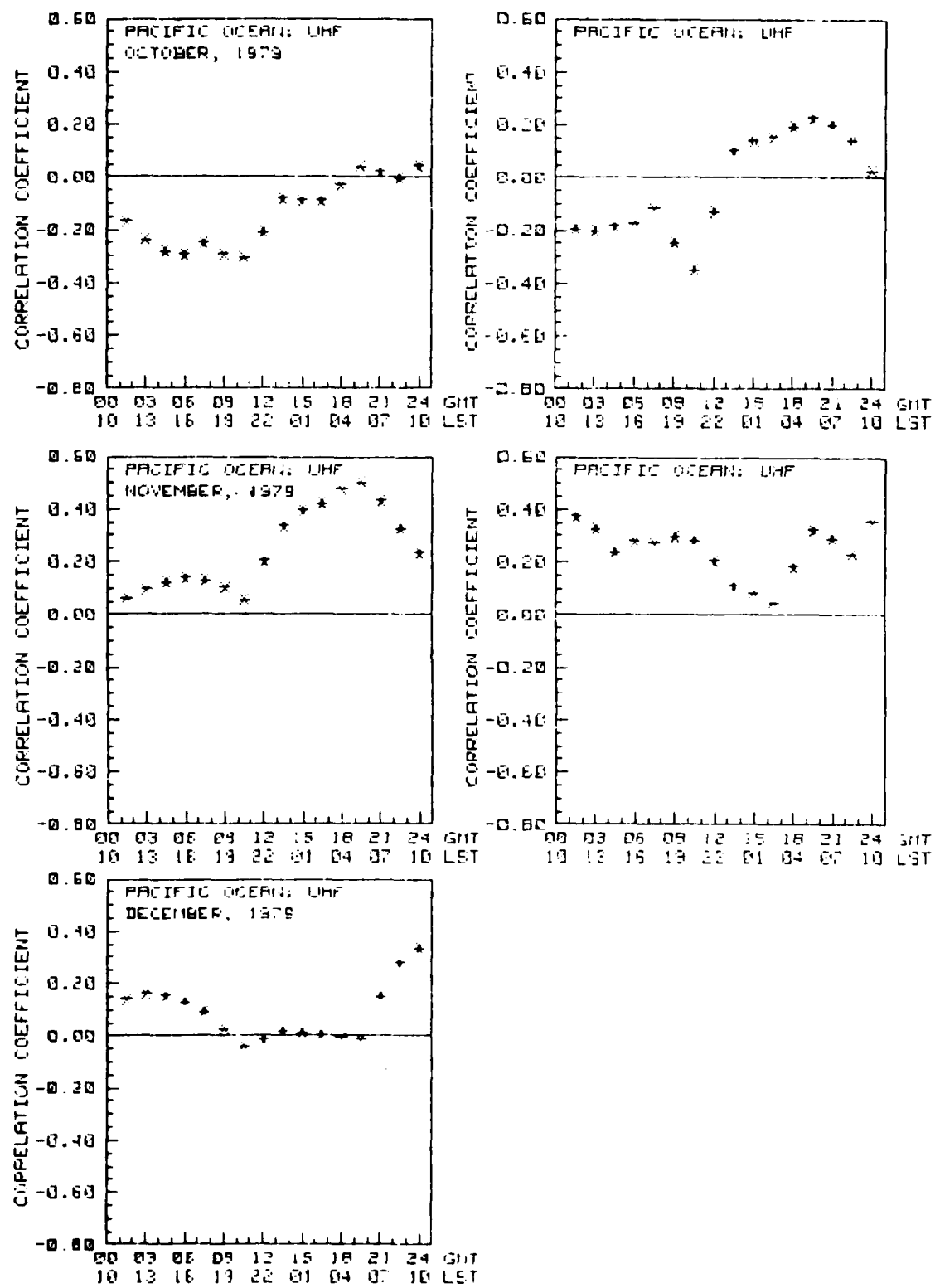


Figure 4. The same as figure 3, but for F3, the Pacific Ocean satellite. (Continued)

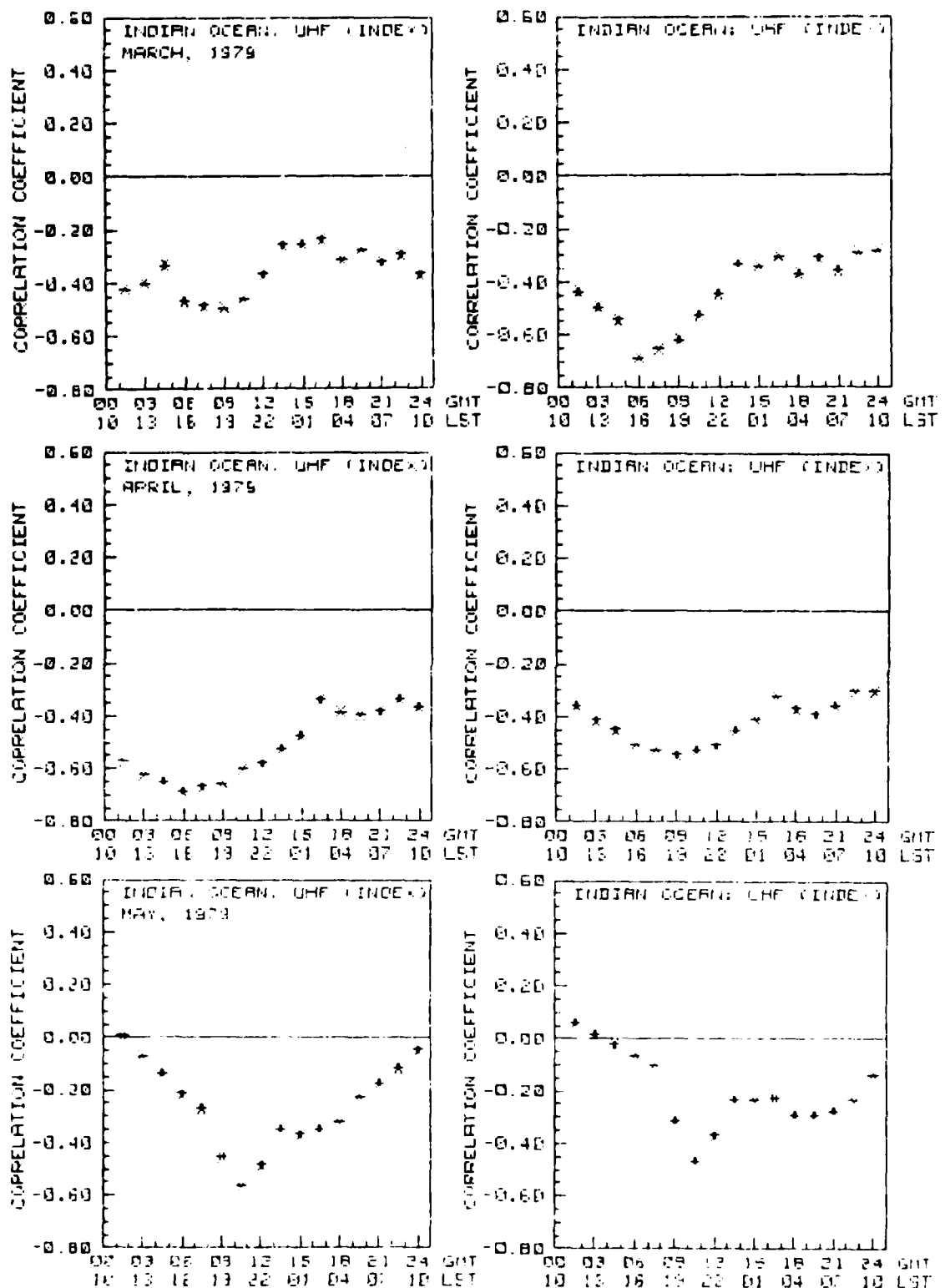


Figure 5. Cross correlations between nightly sums of standard deviation divided by the mean and the 3-hour K<sub>p</sub> indices plotted as a function of the time of the K<sub>p</sub> measurement, using 30-day data samples for F2.

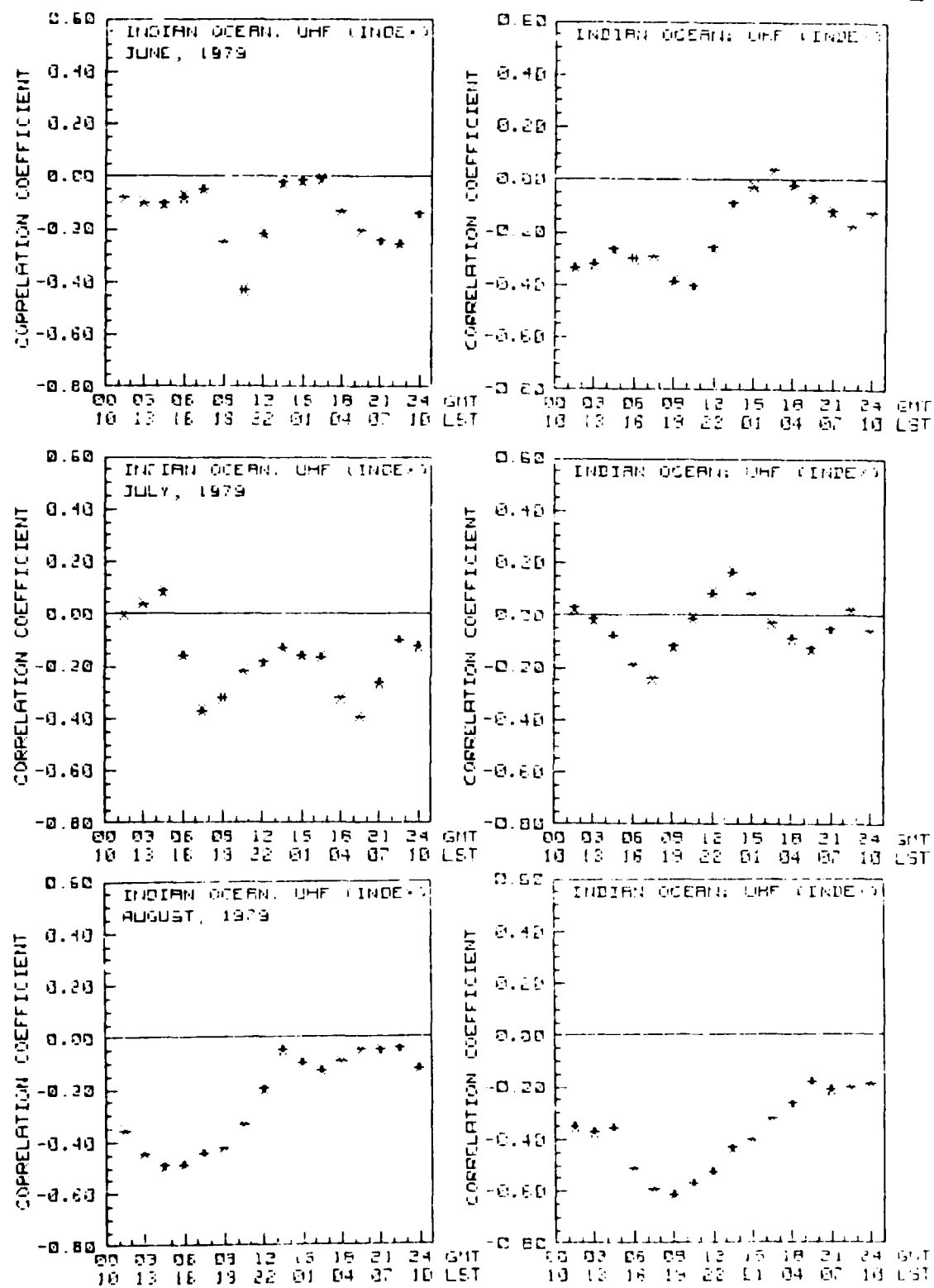


Figure 5. Cross correlations between nightly sums of standard deviation divided by the mean and the 3-hour Kp indices plotted as a function of the time of the Kp measurement, using 30-day data samples for F2. (Continued)

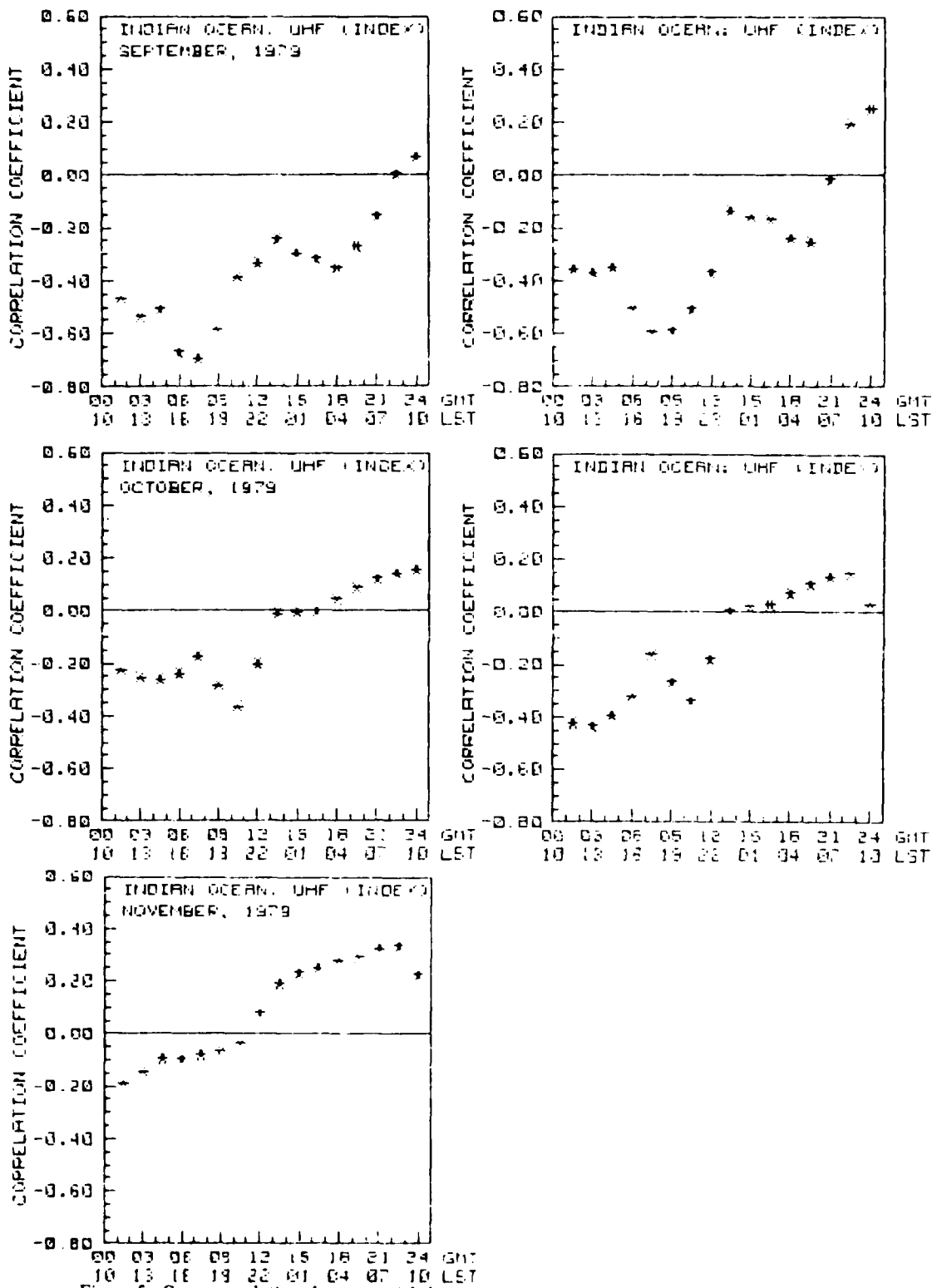


Figure 5. Cross correlations between nightly sums of standard deviation divided by the mean and the 3-hour Kp indices plotted as a function of the time of the Kp measurement, using 30-day data samples for F2. (Continued)

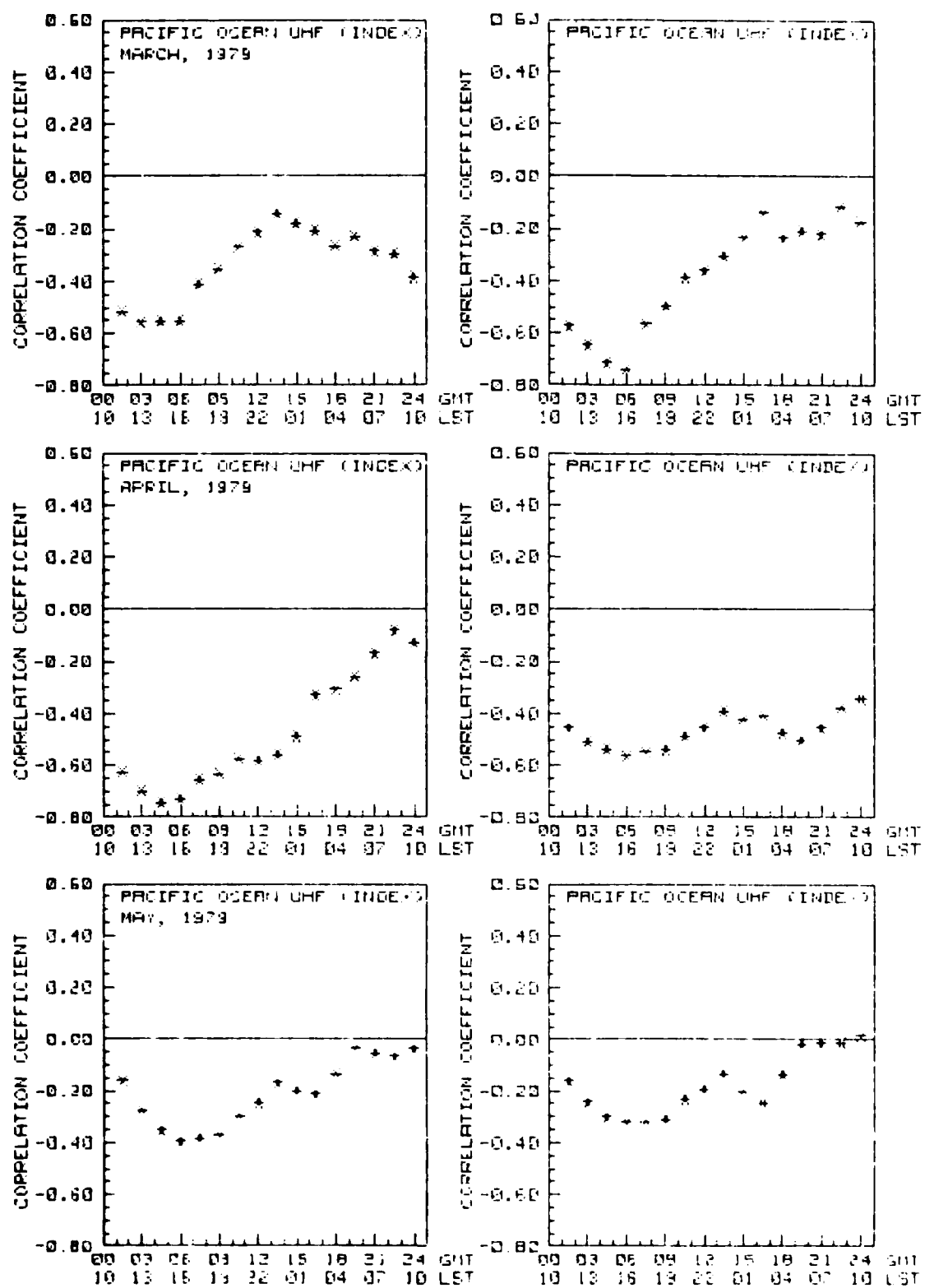


Figure 6. The same as figure 5, but for F3.

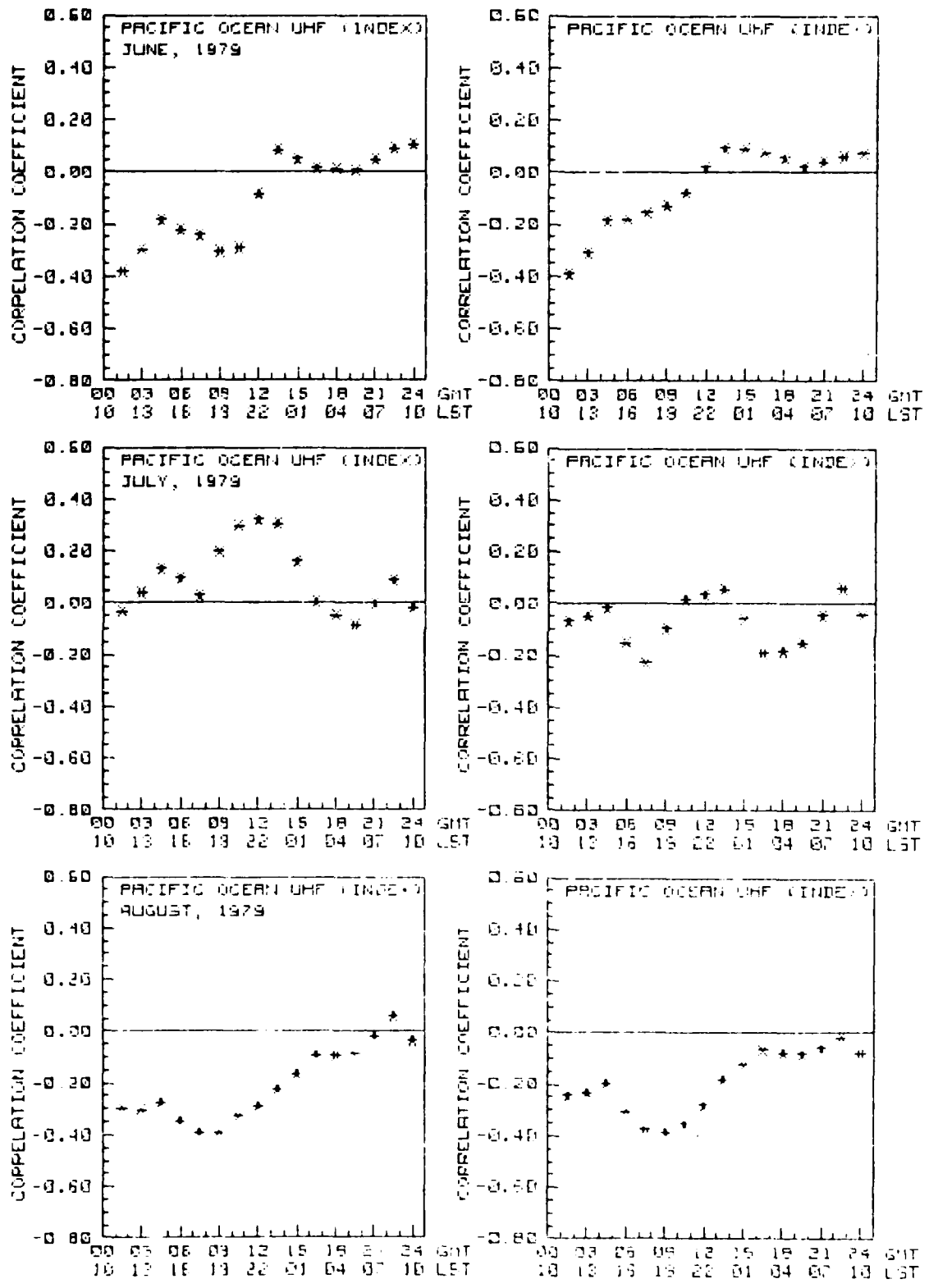


Figure 6. The same as figure 5, but for F3. (Continued)

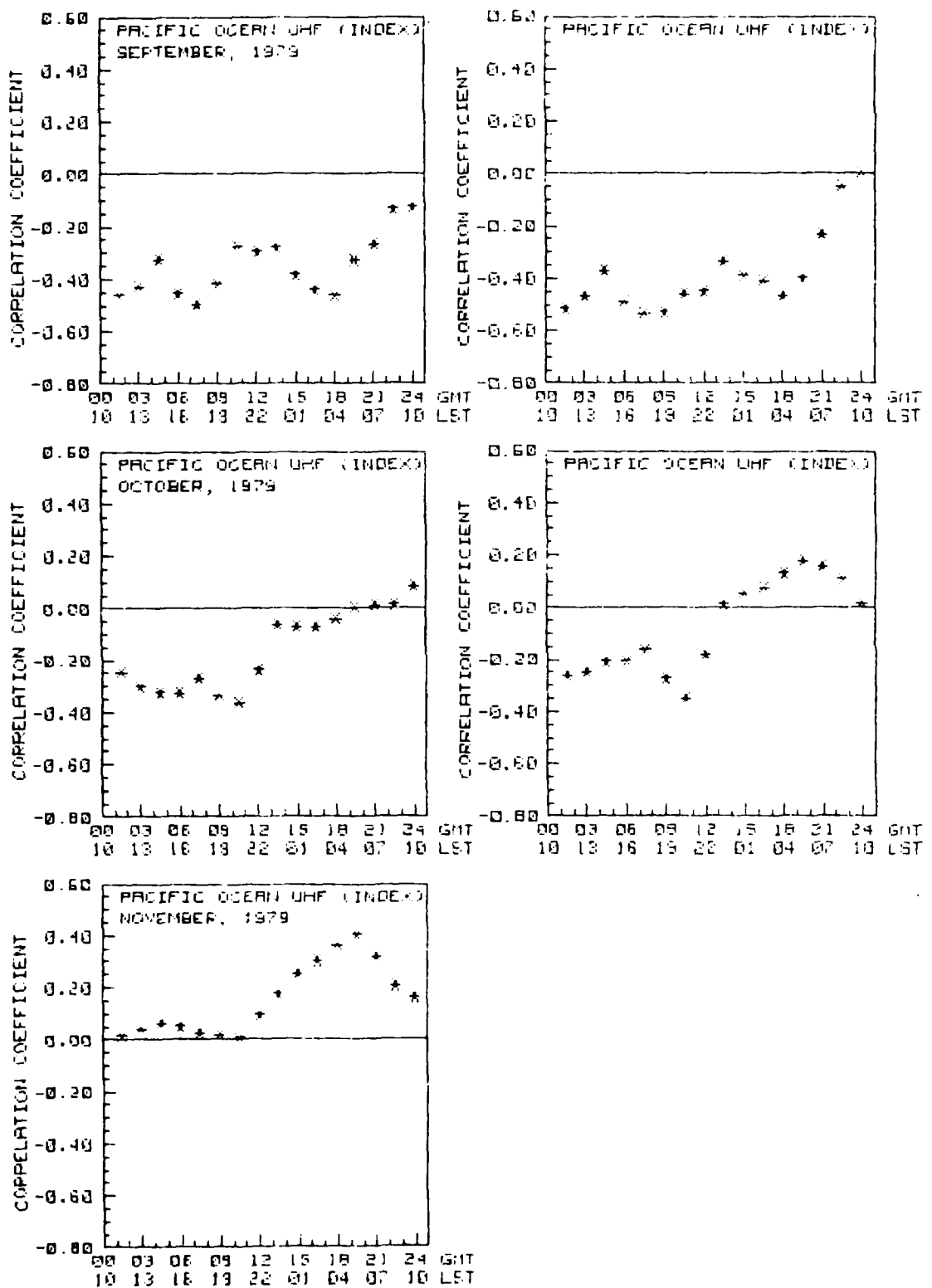


Figure 6. The same as figure 5, but for F3. (Continued)

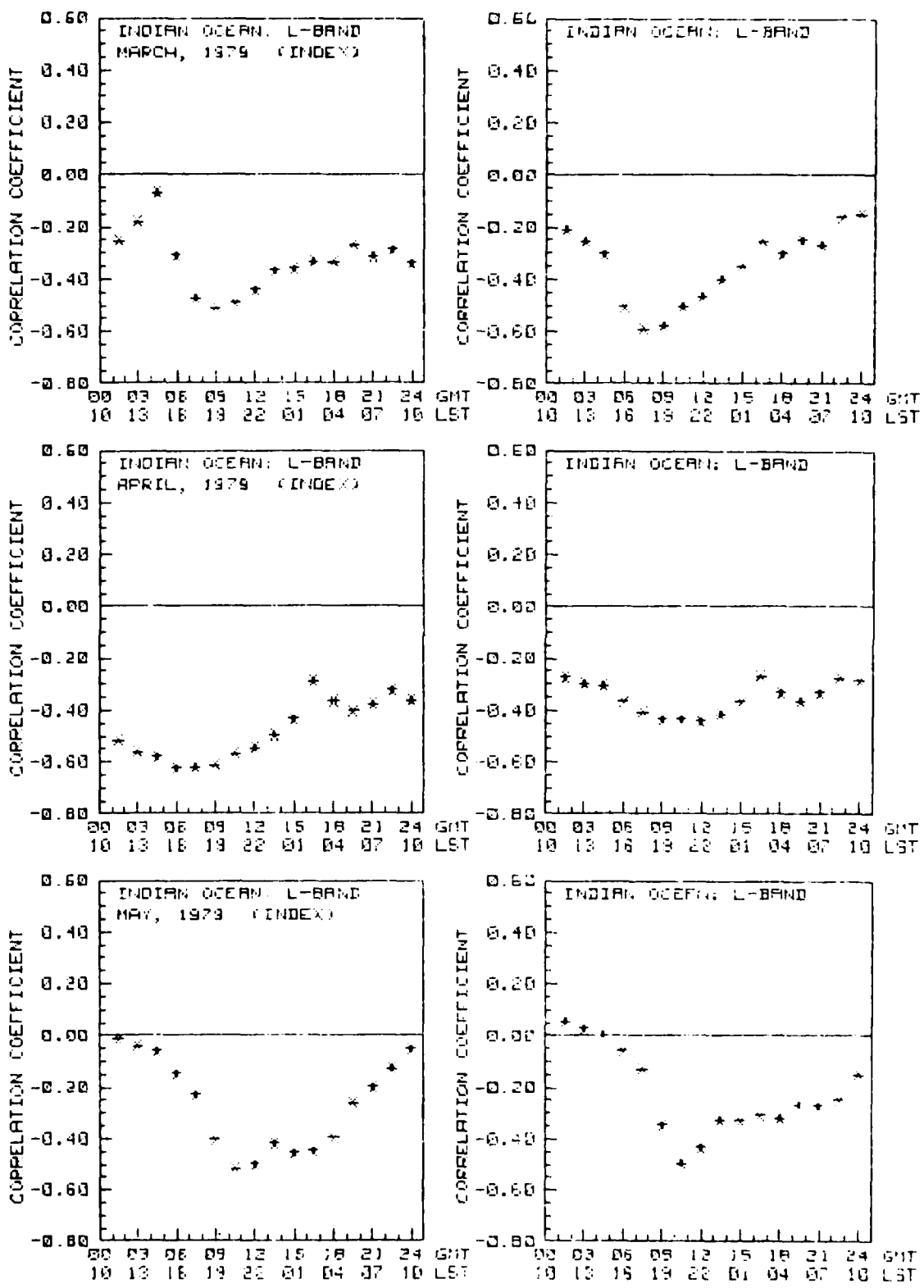


Figure 7. The same as figure 5, but for the L-band signals on F2.

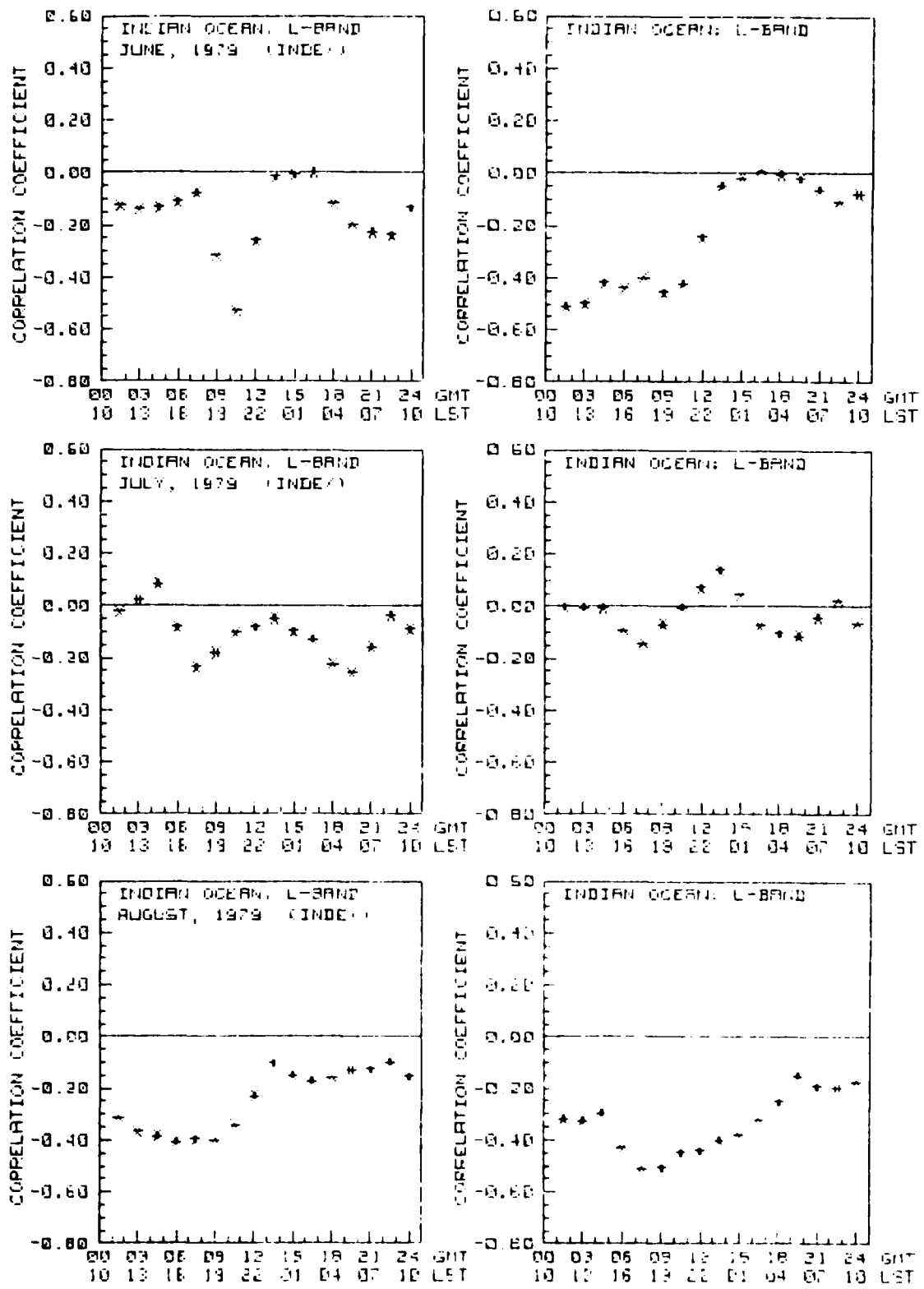


Figure 7. The same as figure 5, but for the L-band signals on F2. (Continued)

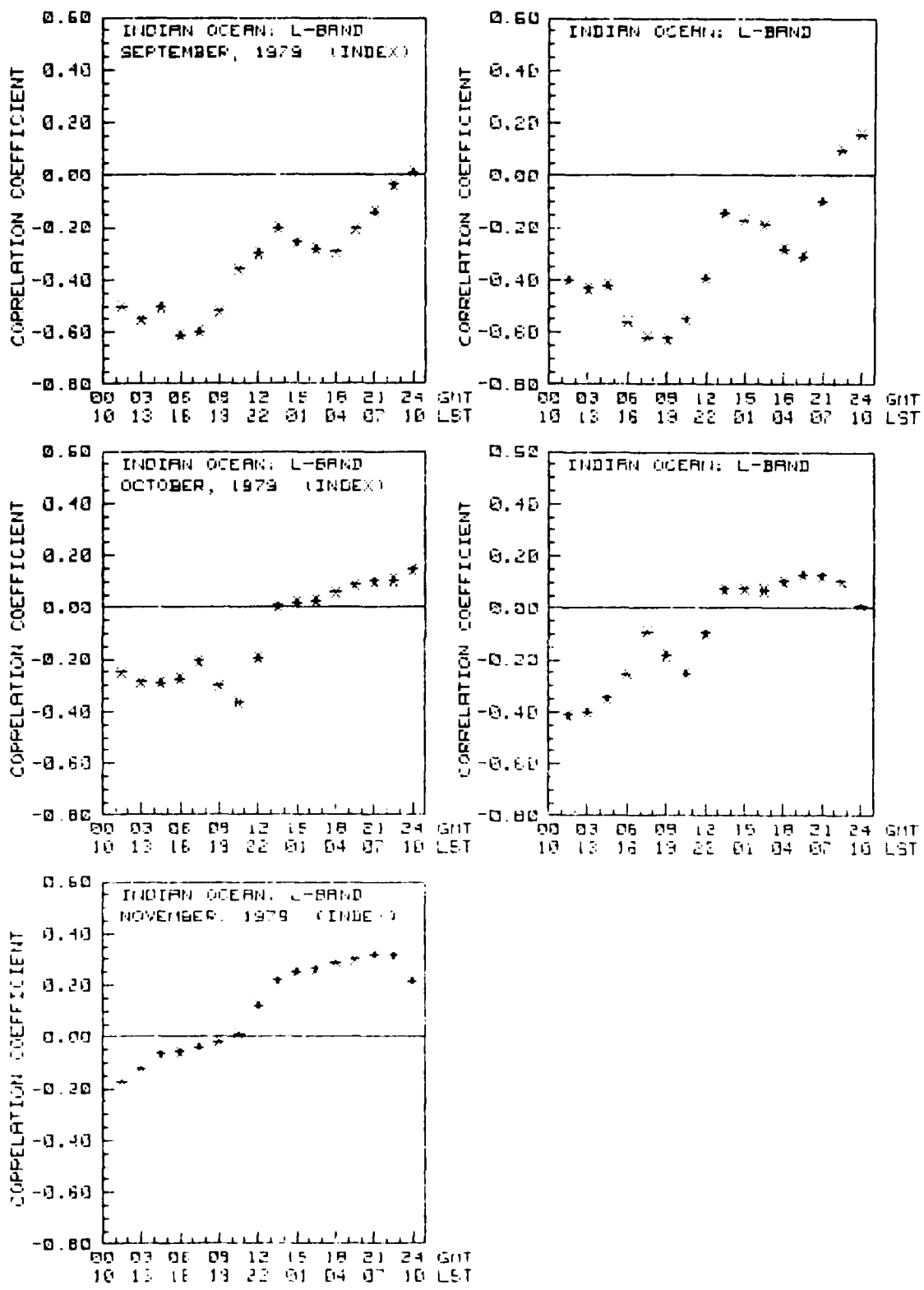


Figure 7. The same as figure 5, but for the L-band signals on F2. (Continued)

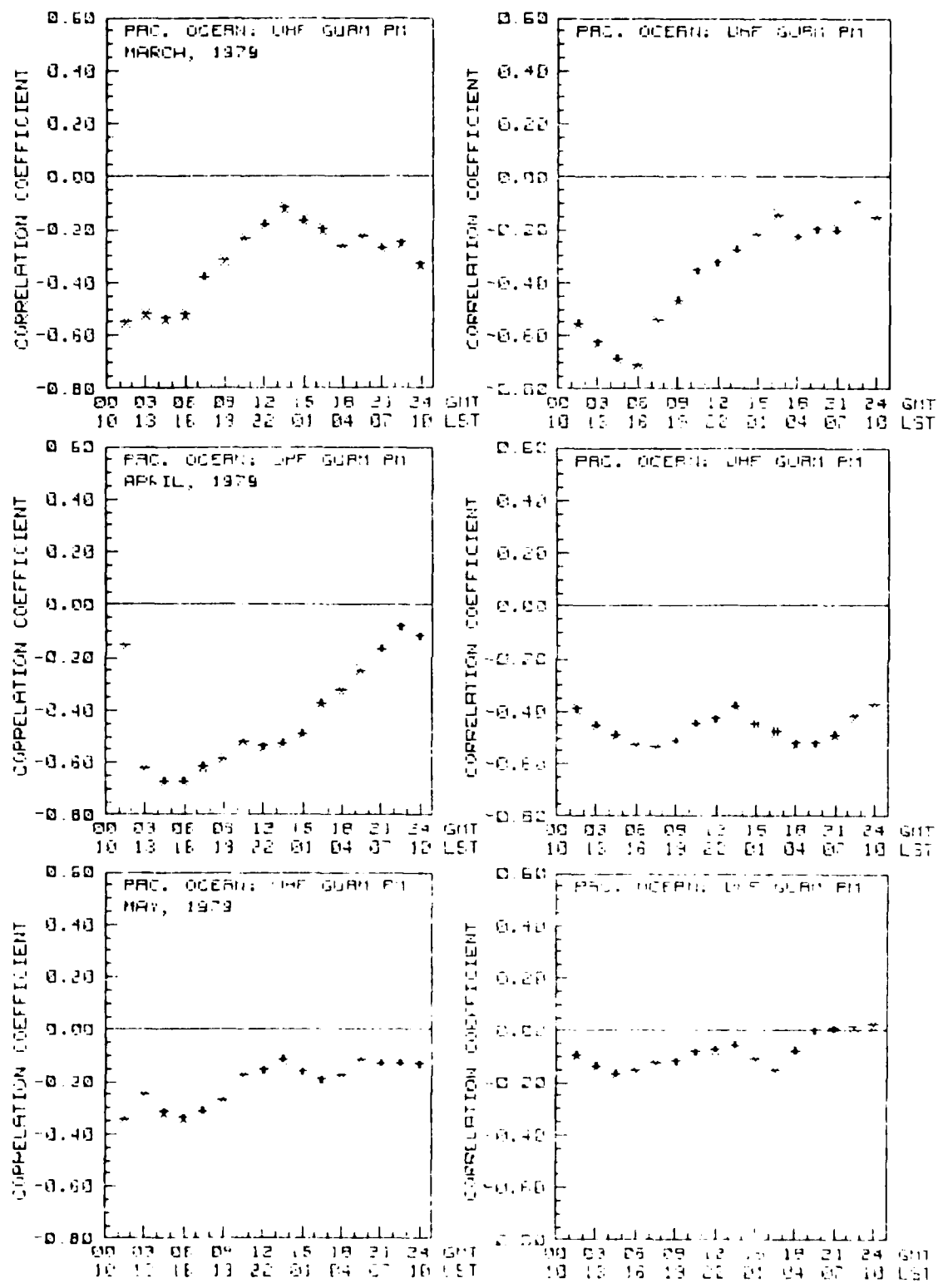


Figure 8. Cross correlations between sums of standard deviation divided by the mean prior to local midnight and the 3-hour Kp indices plotted as a function of the time of the Kp measurement, using 30-day data samples for F3.

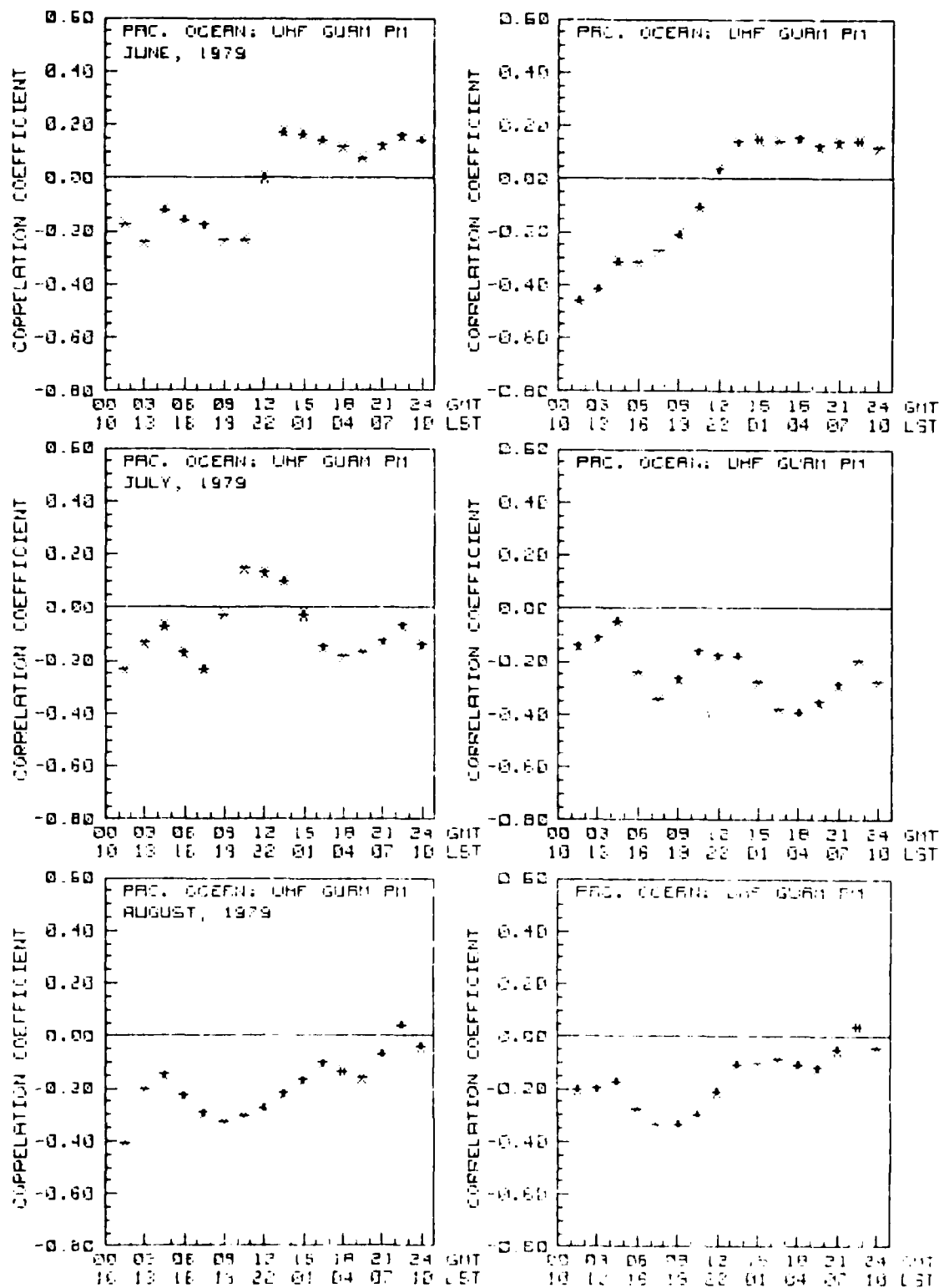


Figure 8. Cross correlations between sums of standard deviation divided by the mean prior to local midnight and the 3-hour Kp indices plotted as a function of the time of the Kp measurement, using 30-day data samples for F3. (Continued)

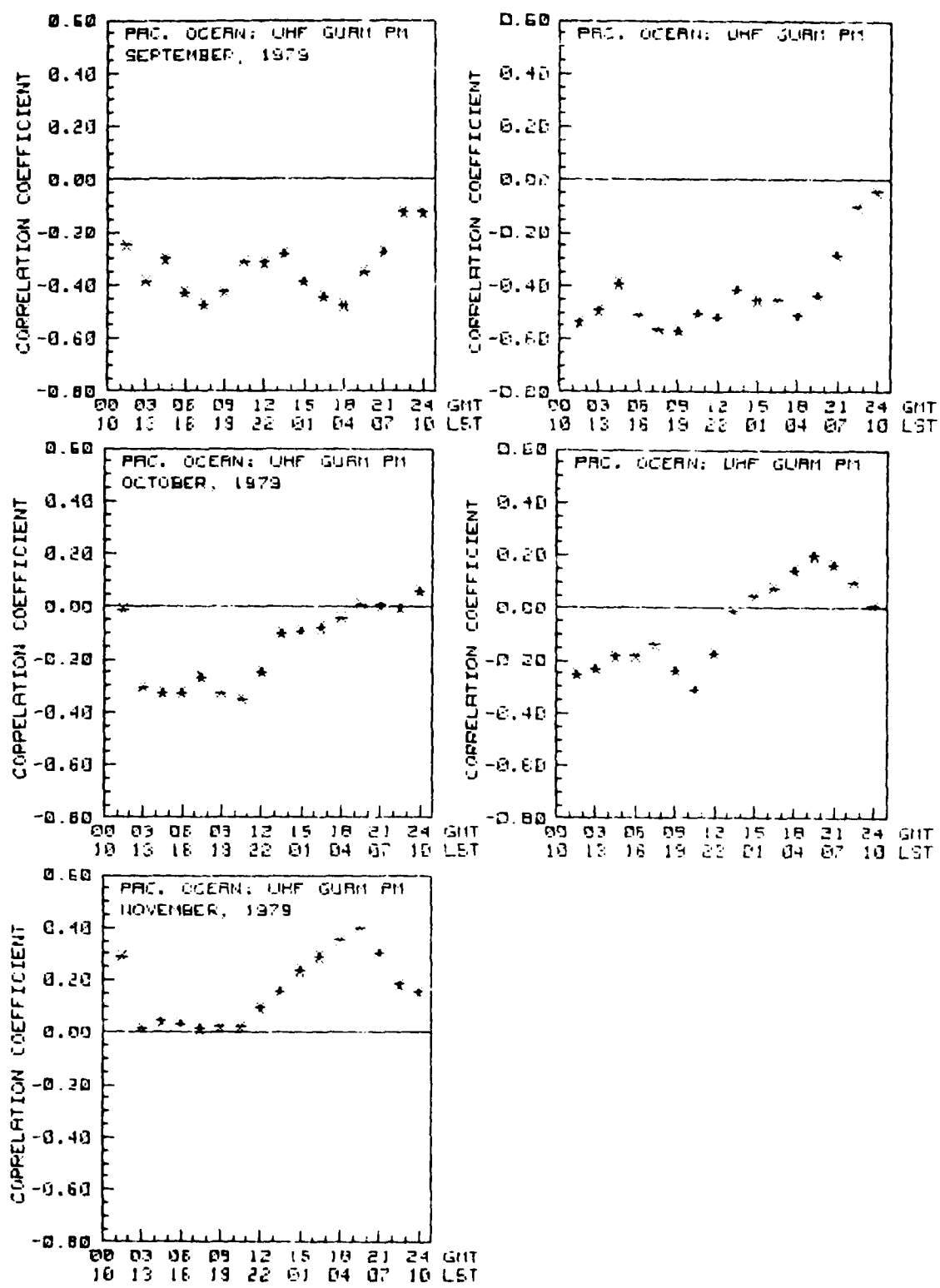


Figure 8. Cross correlations between sums of standard deviation divided by the mean prior to local midnight and the 3-hour Kp indices plotted as a function of the time of the Kp measurement, using 30-day data samples for F3. (Continued)

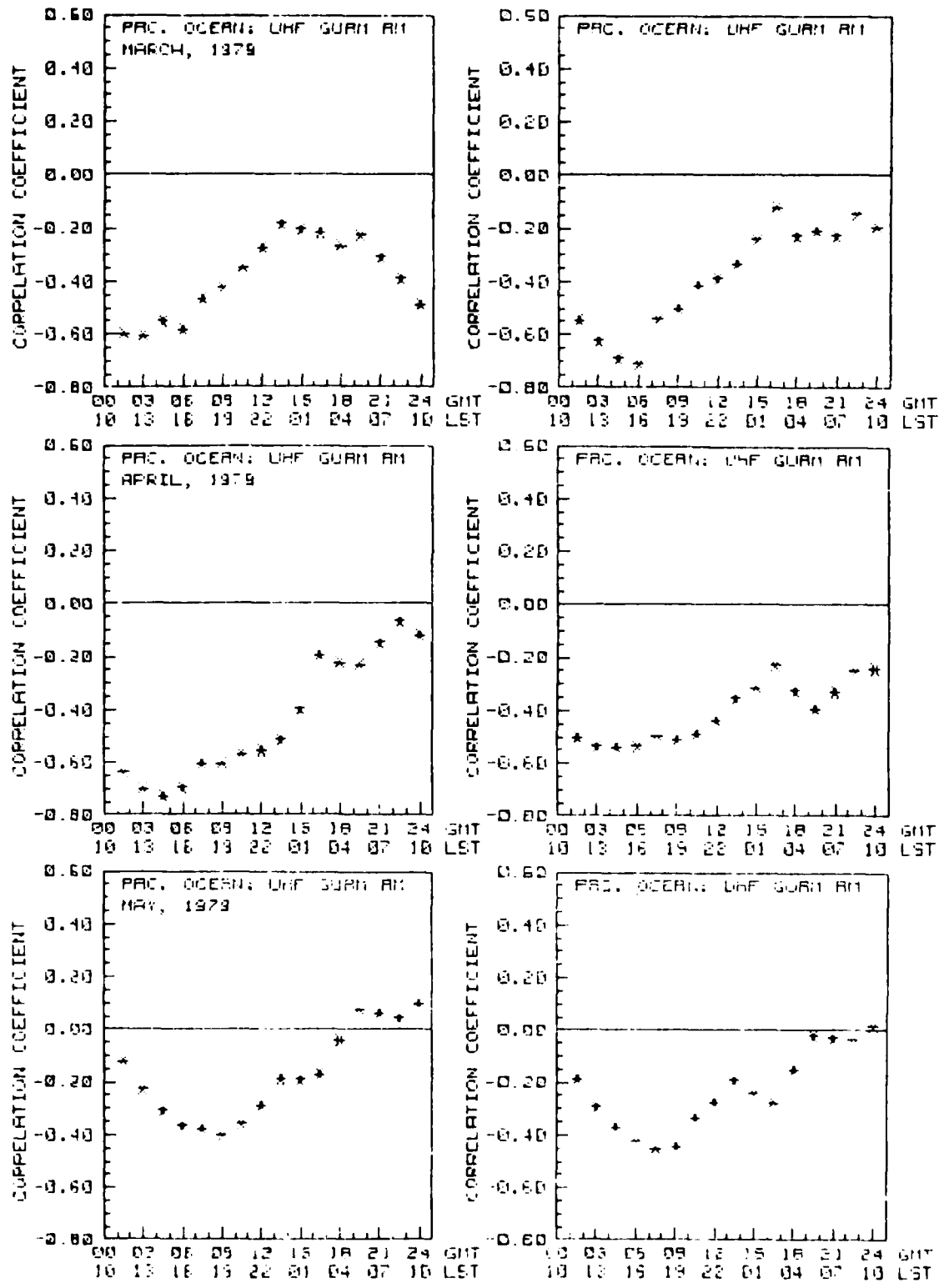


Figure 9. The same as figure 8, but using sums of standard deviation divided by the mean between local midnight and 0300.

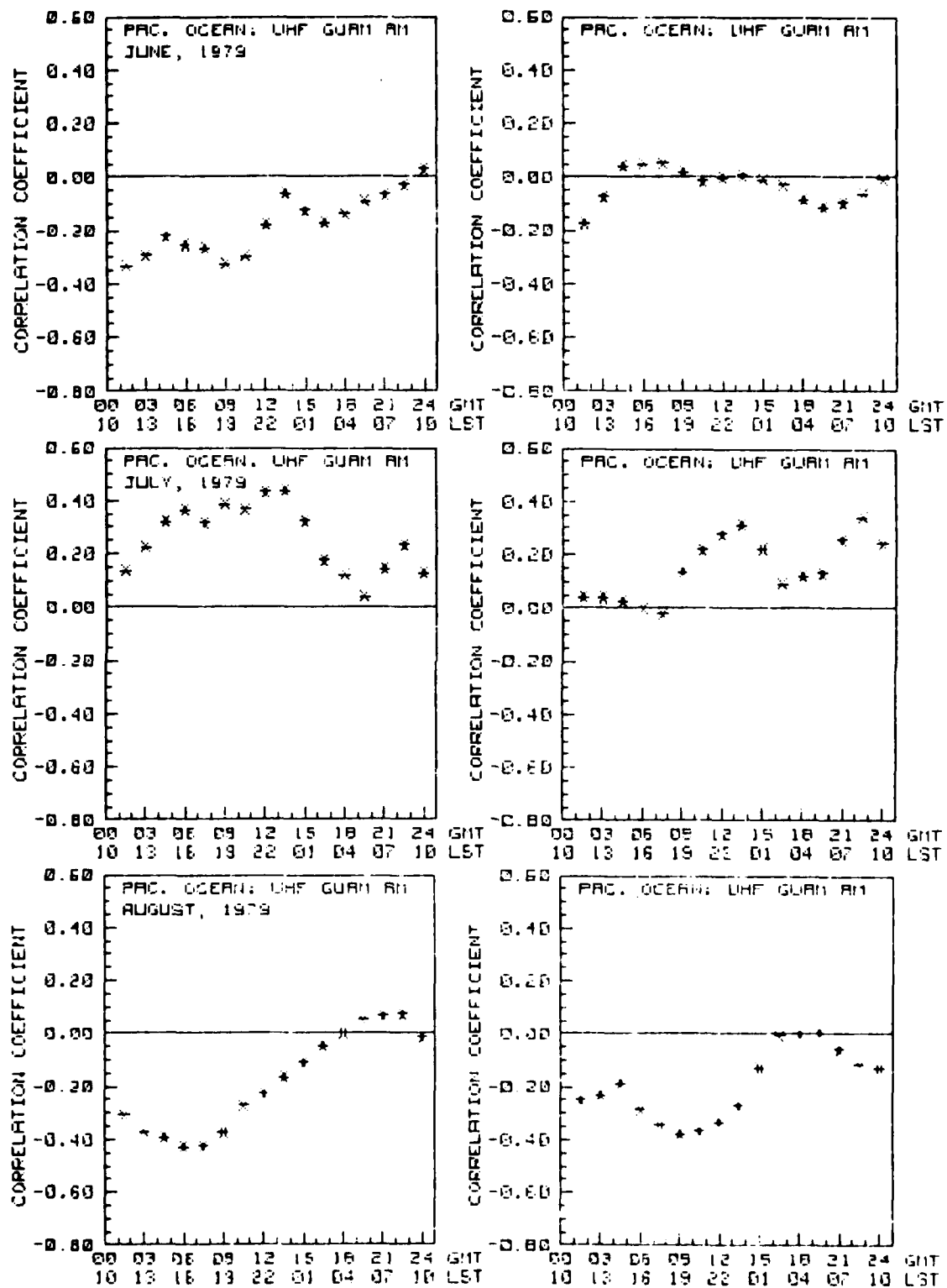


Figure 9. The same as figure 8, but using sums of standard deviation divided by the mean between local midnight and 0300. (Continued)

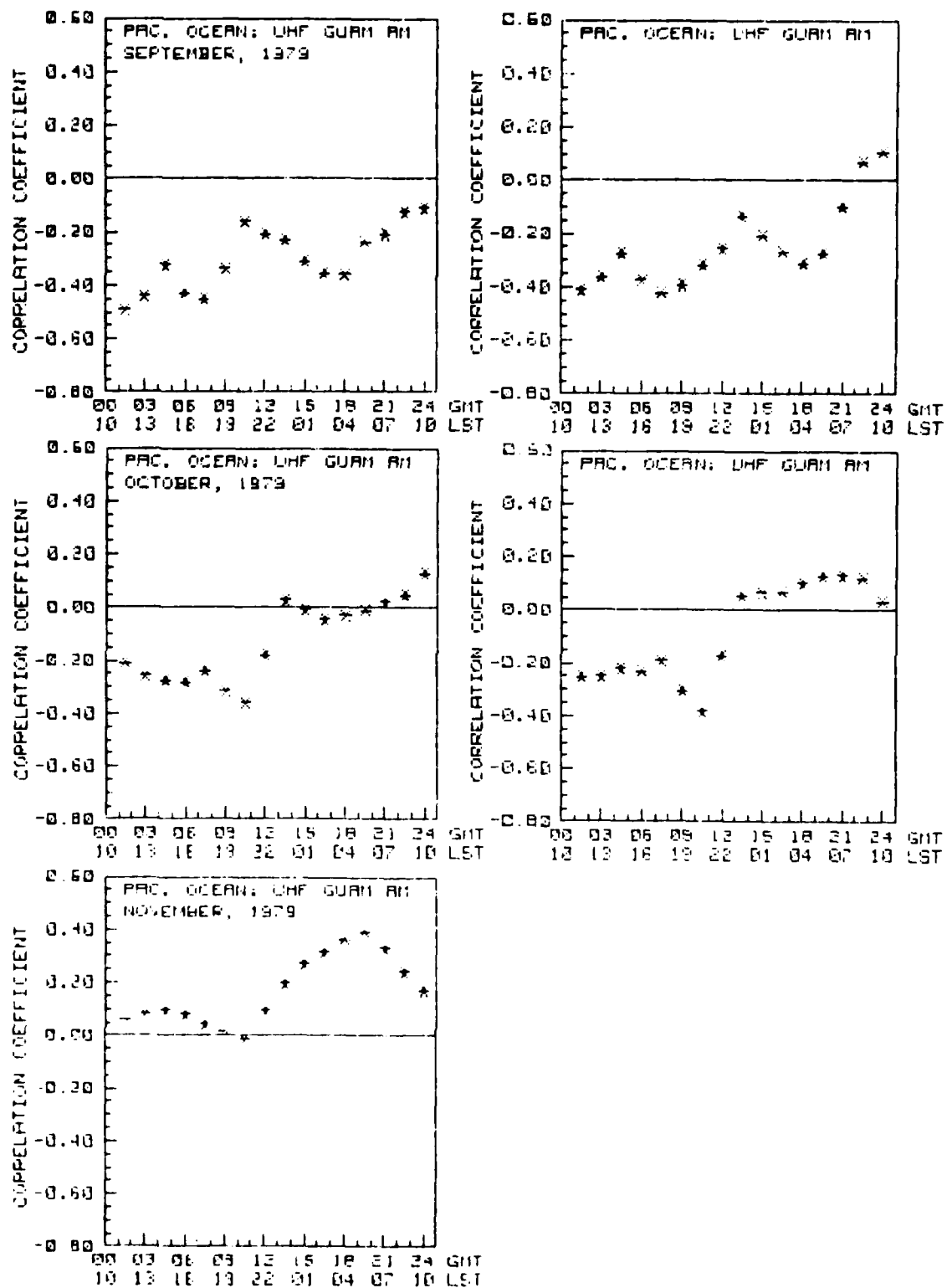


Figure 9. The same as figure 8, but using sums of standard deviation divided by the mean between local midnight and 0300. (Continued)

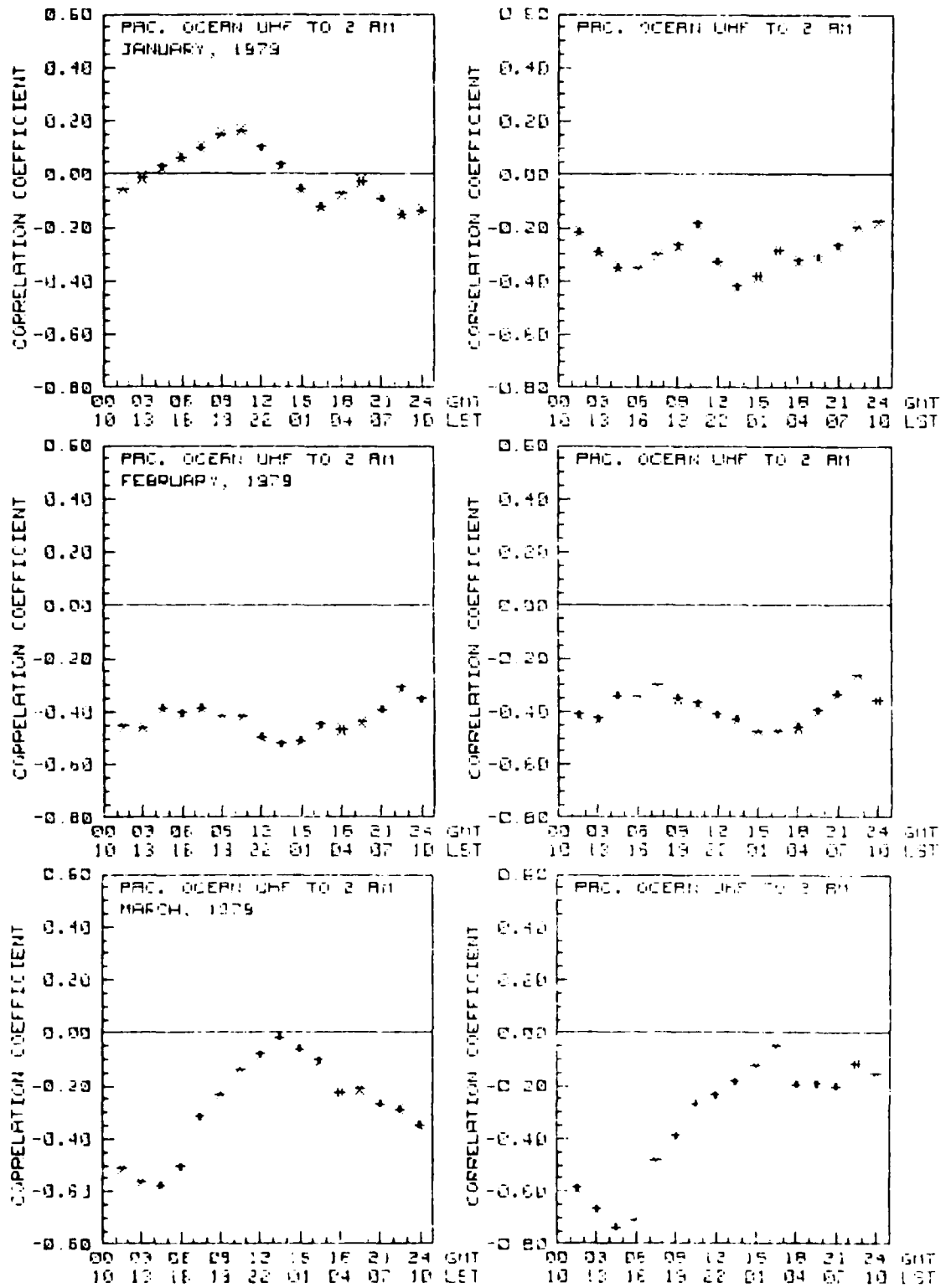


Figure 10. Cross correlations between total hours per night prior to 0200 local time that scintillation fading exceeded 6 dB and the 3-hour K<sub>p</sub> indices plotted as a function of the time of the K<sub>p</sub> measurement, using 30-day data samples for F3.

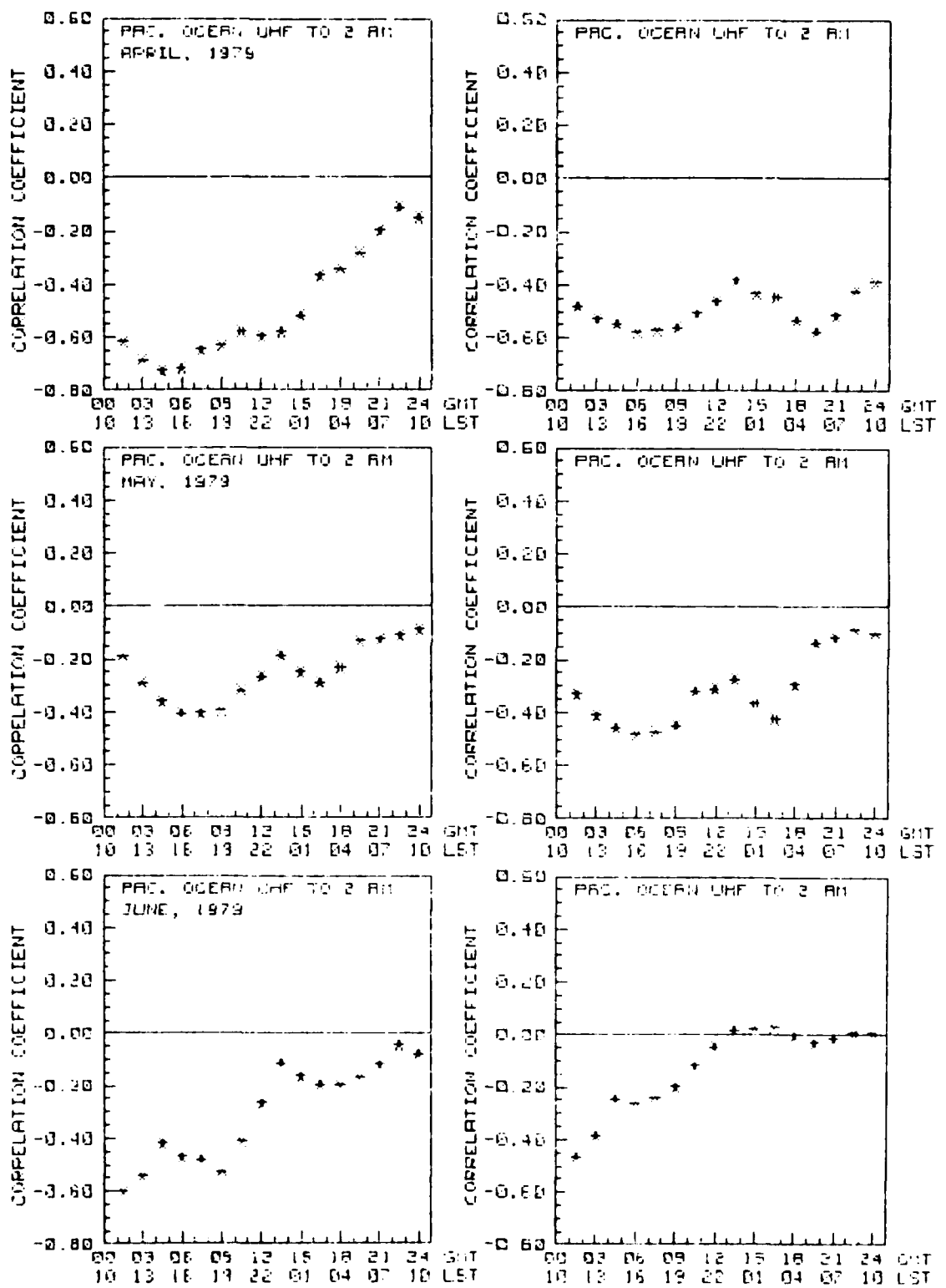


Figure 10. Cross correlations between total hours per night prior to 0200 local time that scintillation fading exceeded 6 dB and the 3-hour  $K_p$  indices plotted as a function of the time of the  $K_p$  measurement, using 30-day data samples for F3. (Continued)

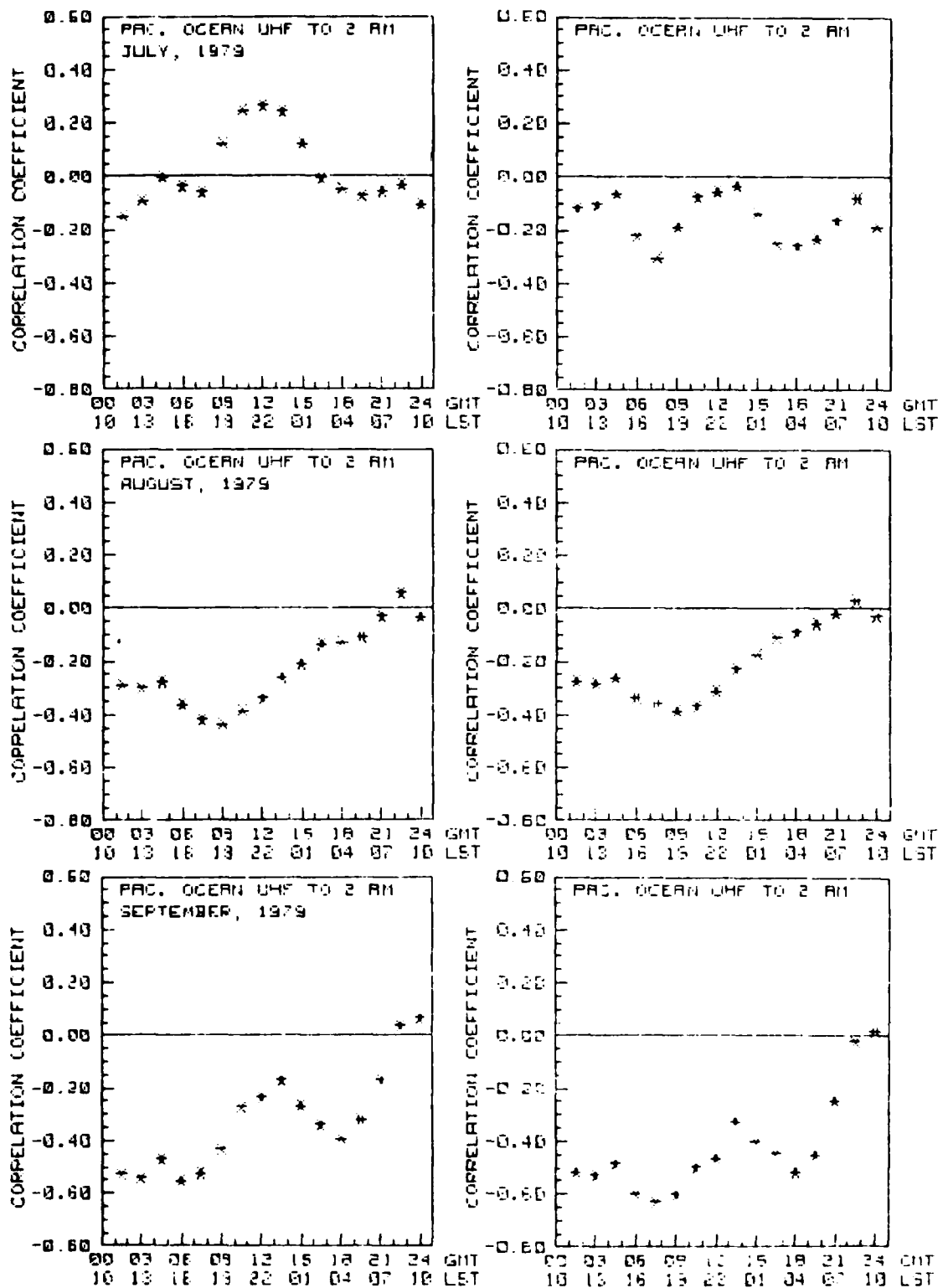


Figure 10. Cross correlations between total hours per night prior to 0200 local time that scintillation fading exceeded 6 dB and the 3-hour Kp indices plotted as a function of the time of the Kp measurement, using 30-day data samples for F3. (Continued)

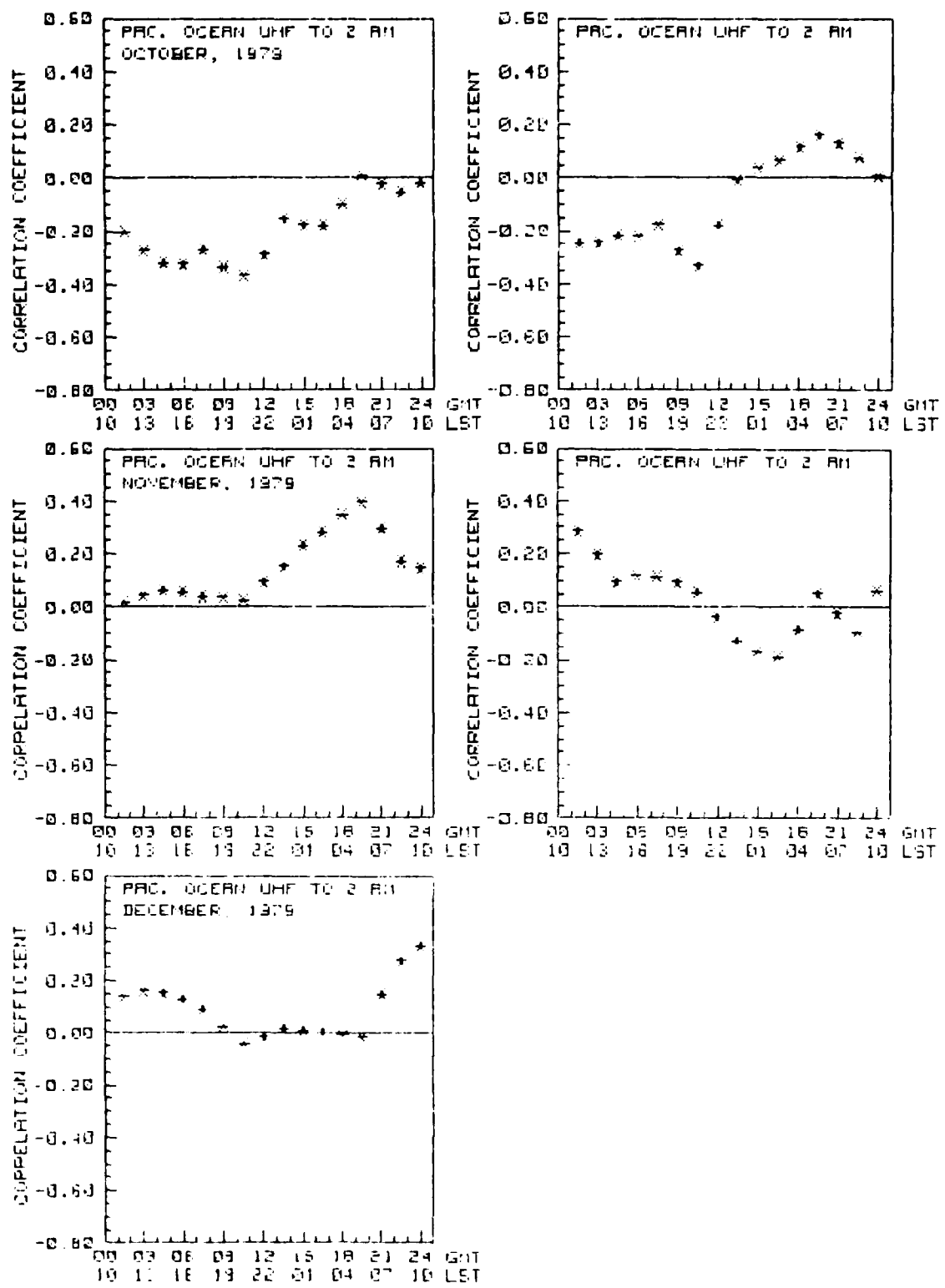


Figure 10. Cross correlations between total hours per night prior to 0200 local time that scintillation fading exceeded 6 dB and the 3-hour K<sub>p</sub> indices plotted as a function of the time of the K<sub>p</sub> measurement, using 30-day data samples for F3. (Continued)

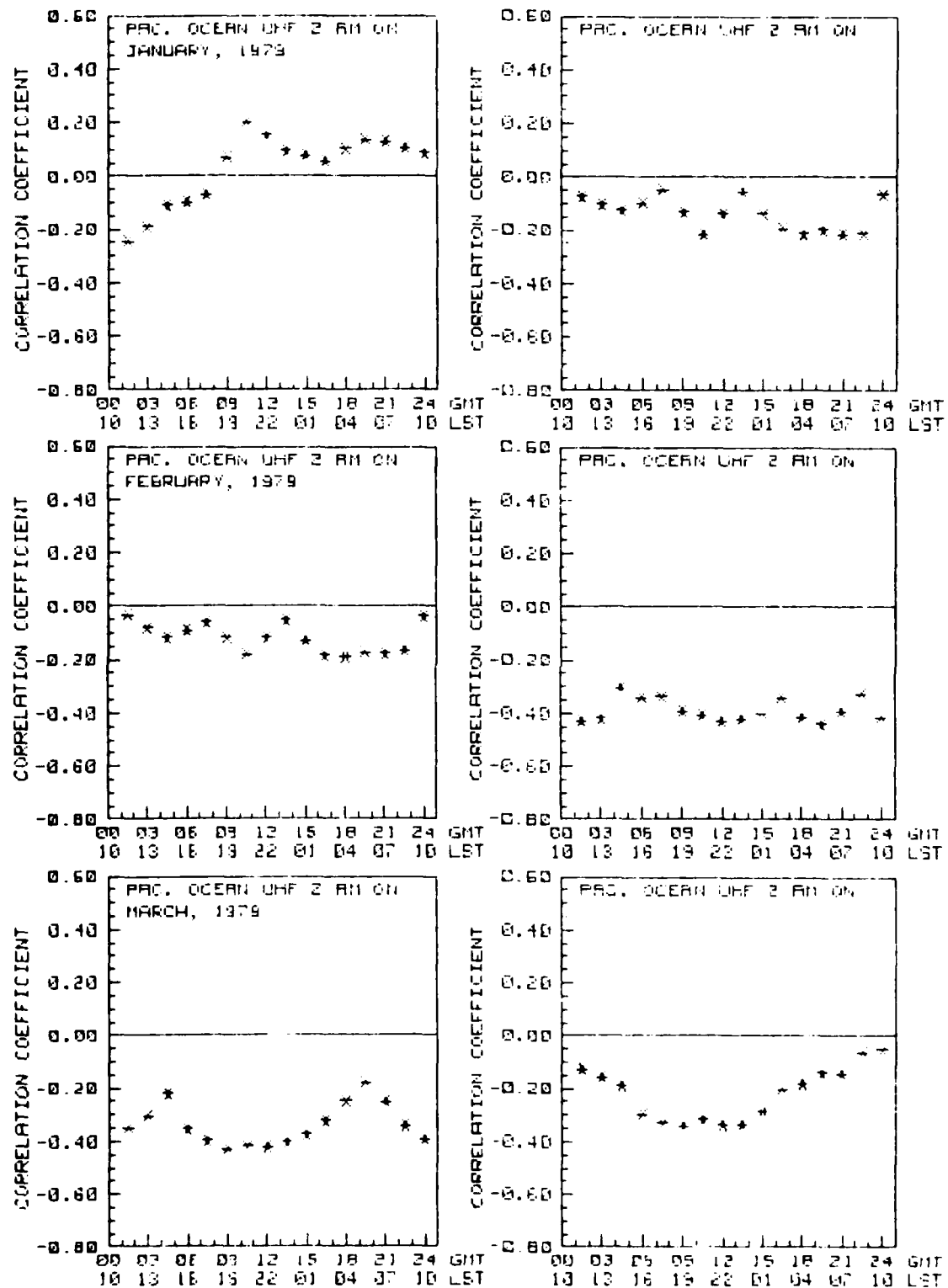


Figure 11. The same as figure 10, but using total hours per night after 0200 local time that scintillation fading exceeded 6 dB.

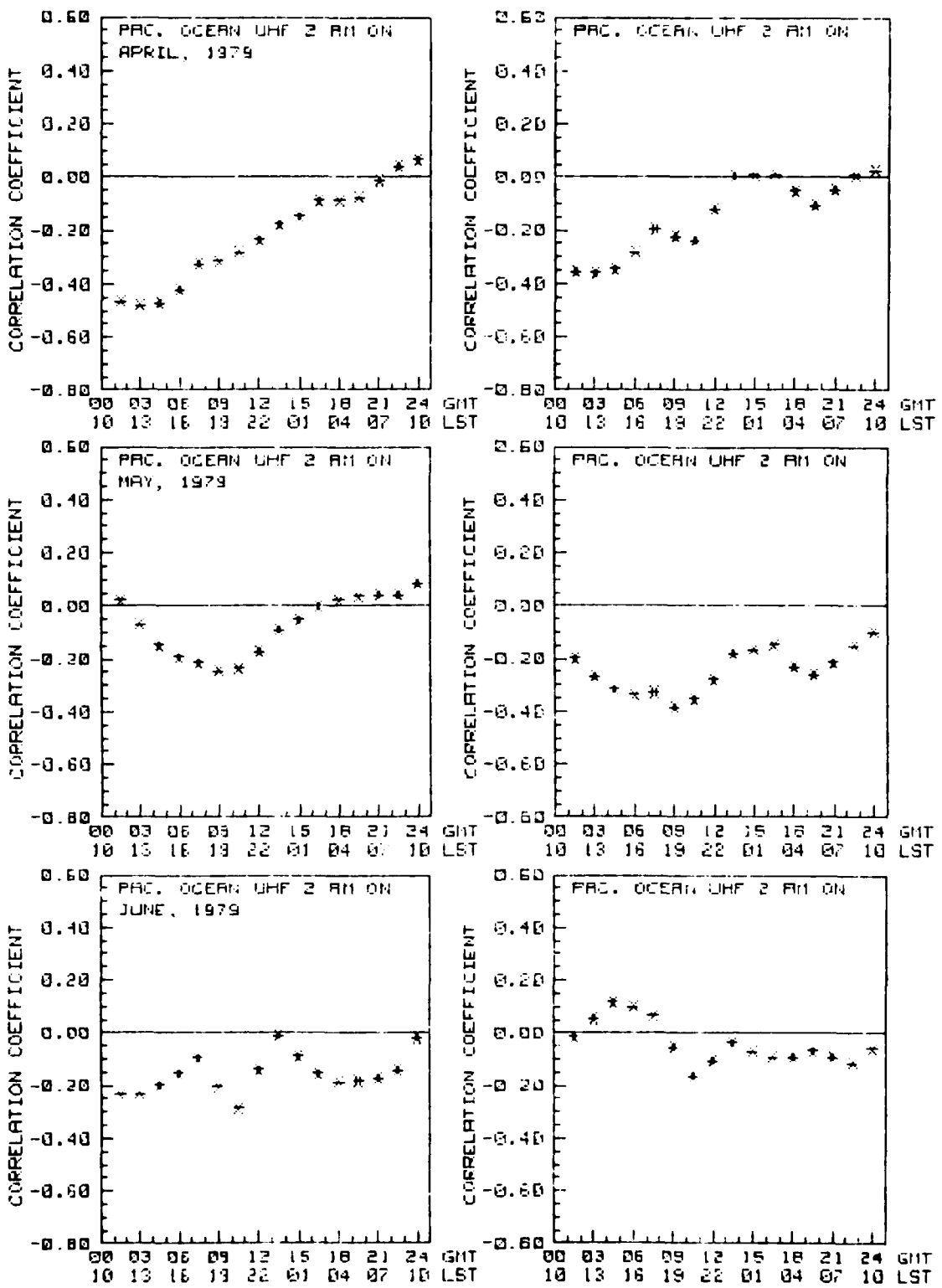


Figure 11. The same as figure 10, but using total hours per night after 0200 local time that scintillation fading exceeded 6 dB. (Continued)

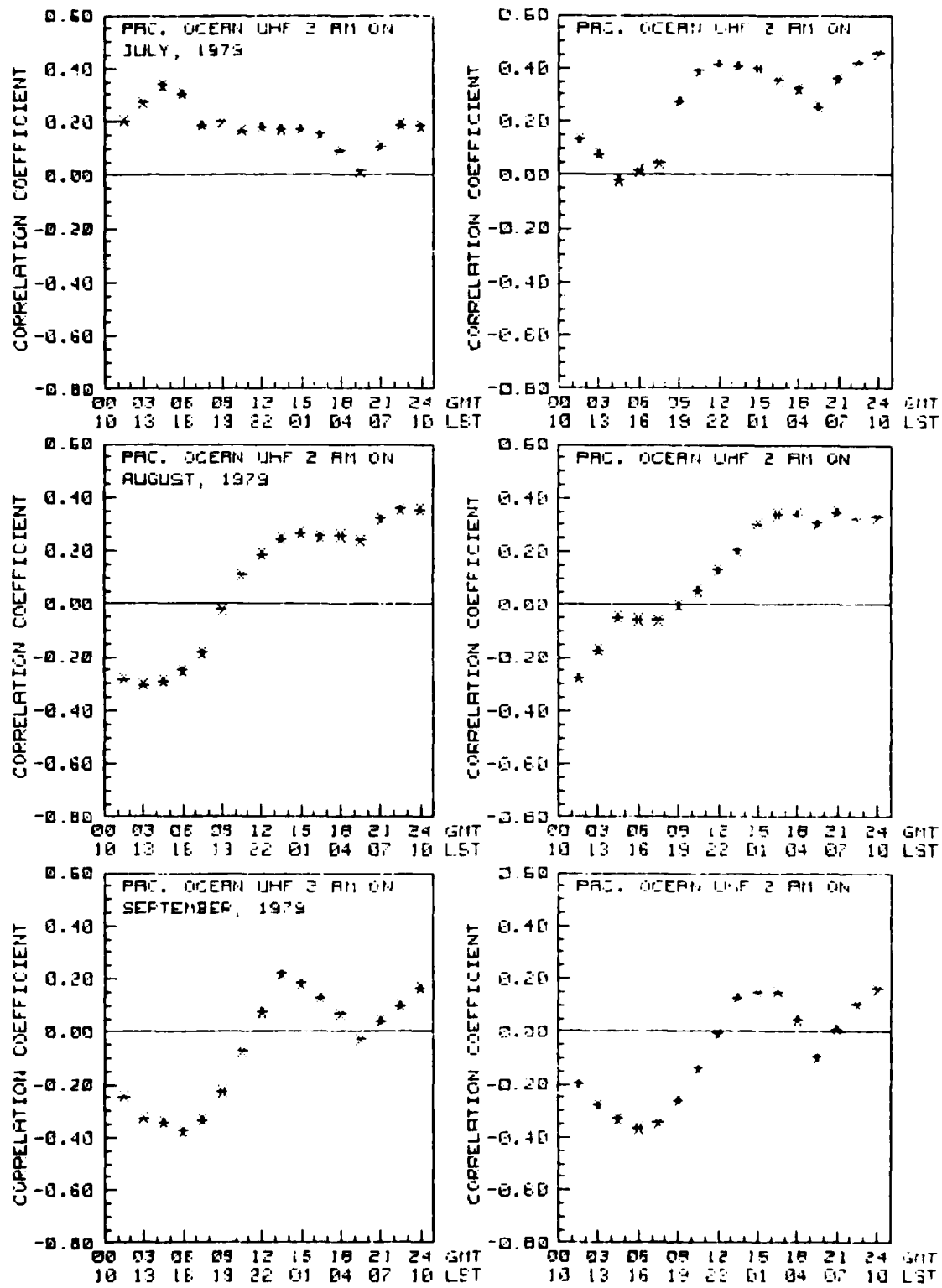


Figure 11. The same as figure 10, but using total hours per night after 0200 local time that scintillation fading exceeded 6 dB. (Continued)

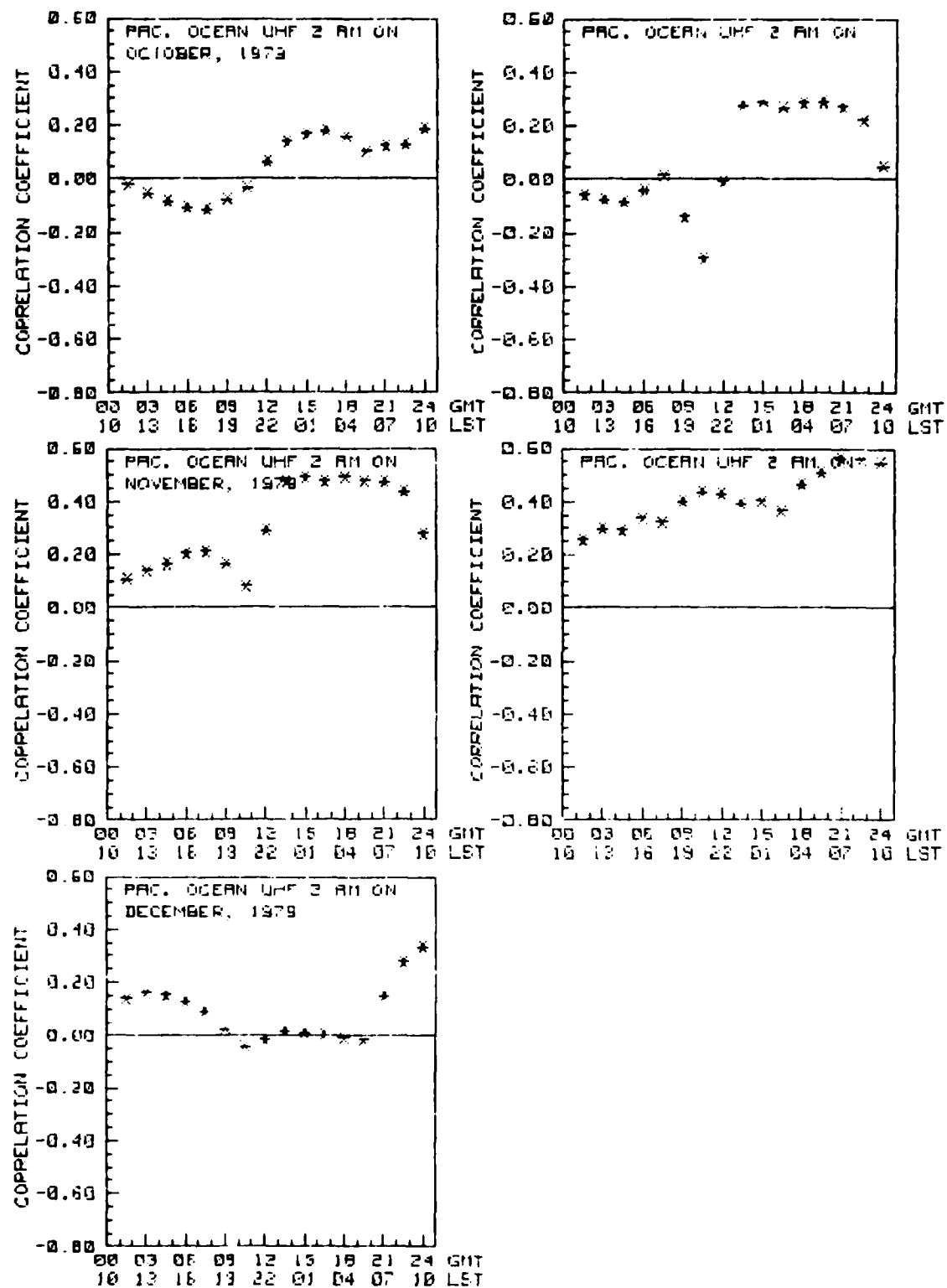


Figure 11. The same as figure 10, but using total hours per night after 0200 local time that scintillation fading exceeded 6 dB. (Continued)

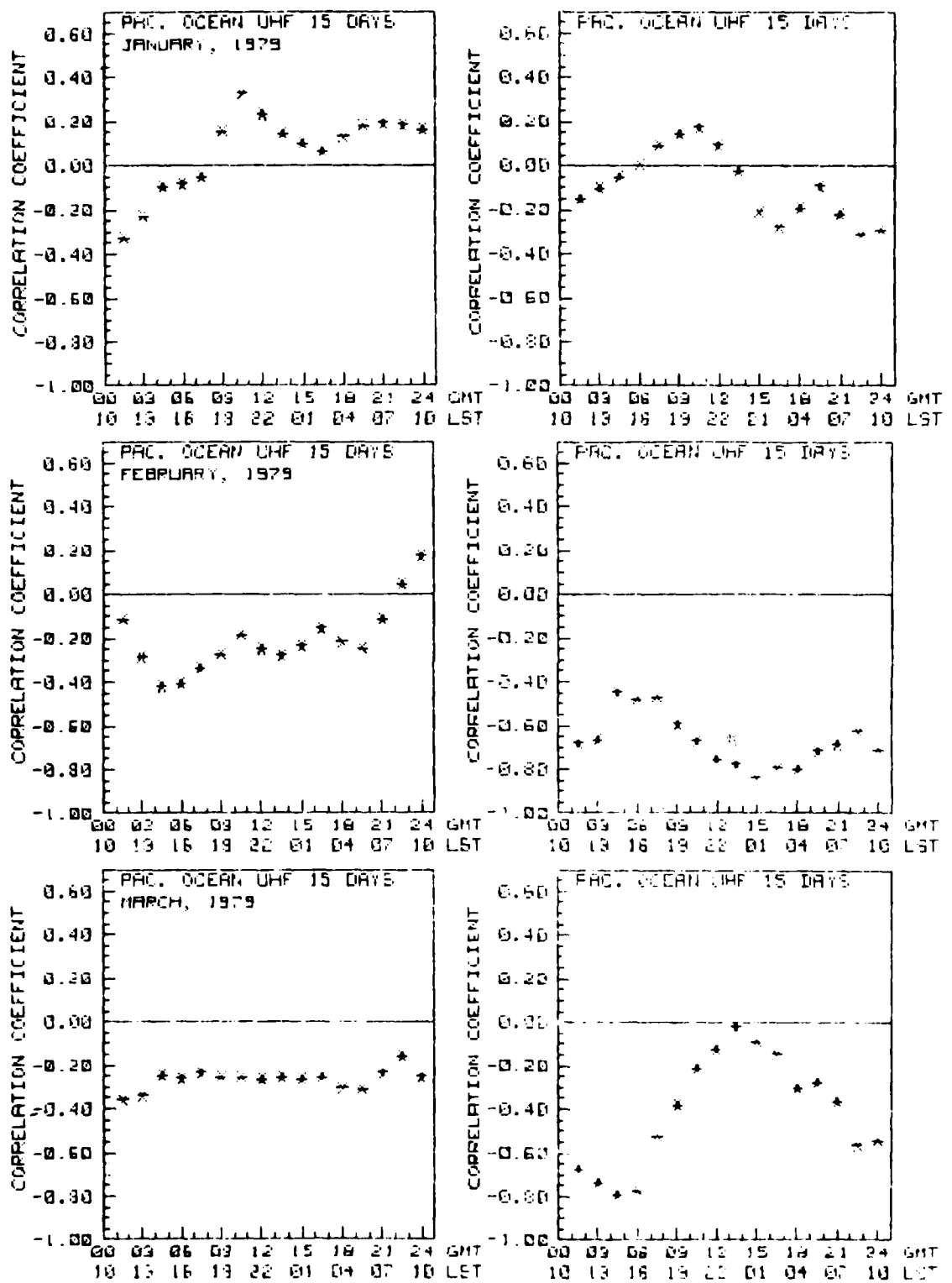


Figure 12. Cross correlations between total hours per night that scintillation fading exceeded 6 dB and the 3-hour K<sub>p</sub> indices plotted as a function of the time of the K<sub>p</sub> measurement, using 15-day data samples for F3.

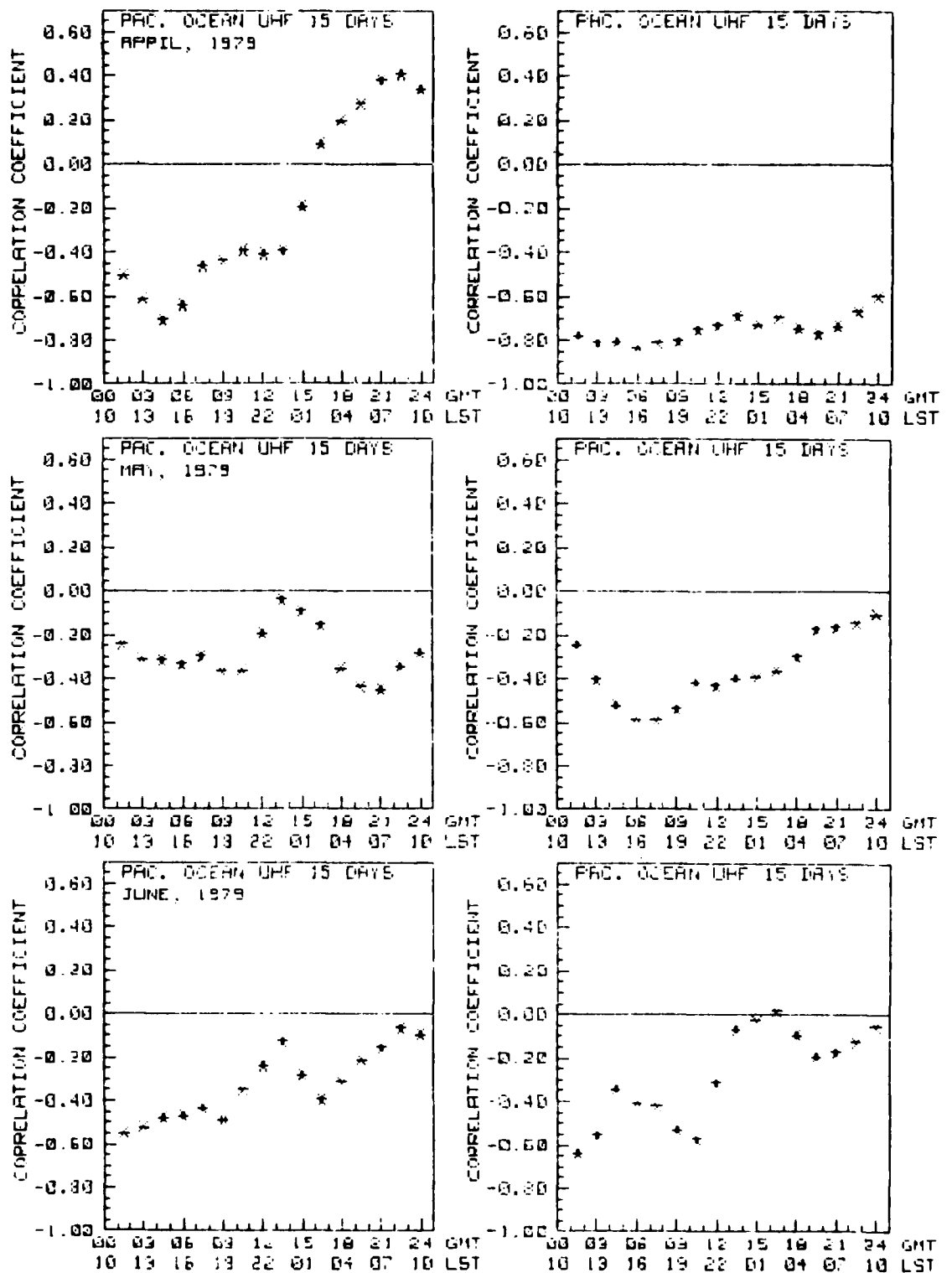


Figure 12. Cross correlations between total hours per night that scintillation fading exceeded 6 dB and the 3-hour K<sub>p</sub> indices plotted as a function of the time of the K<sub>p</sub> measurement, using 15-day data samples for F3. (Continued)

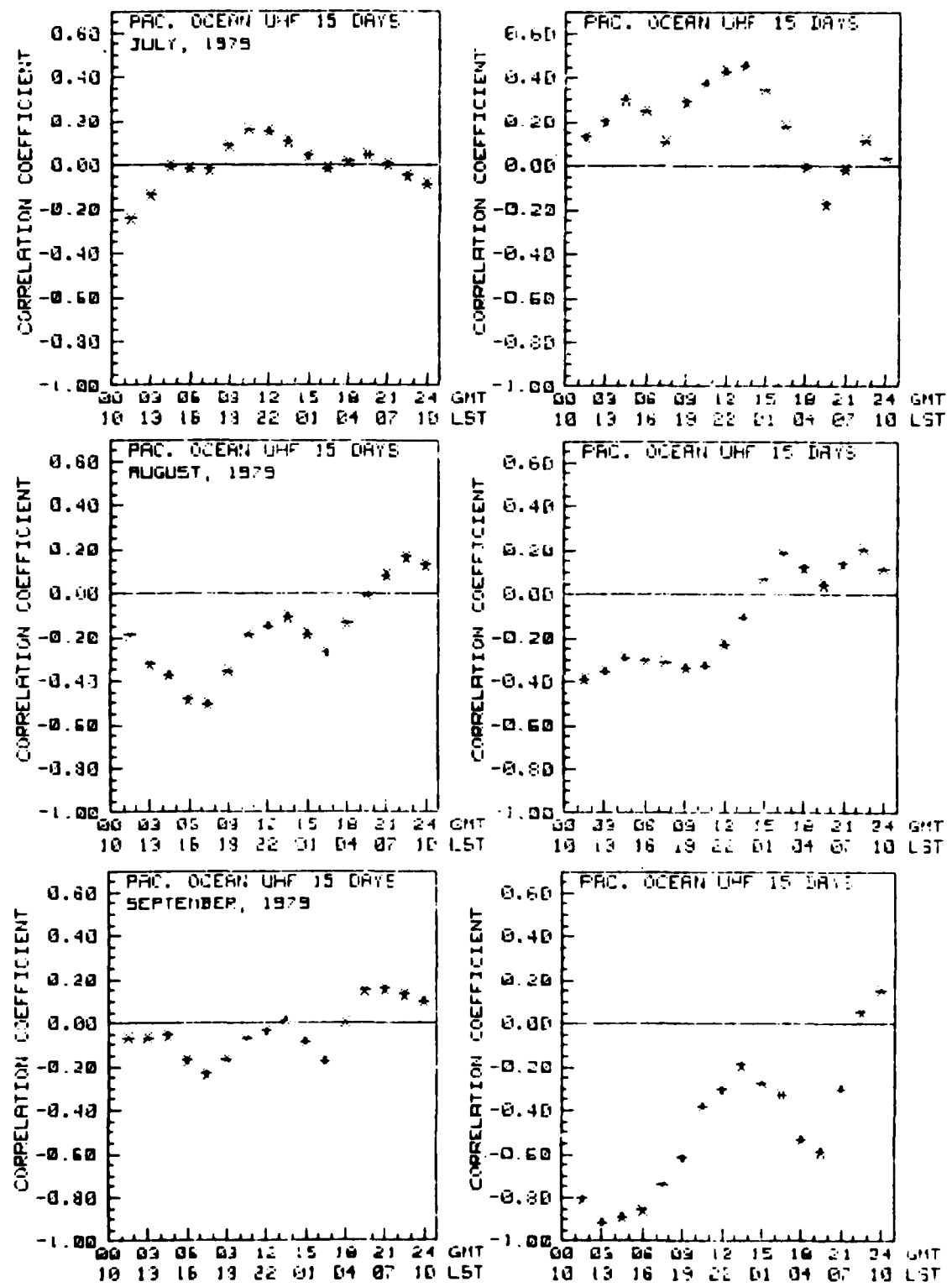


Figure 12. Cross correlations between total hours per night that scintillation fading exceeded 6 dB and the 3-hour K<sub>p</sub> indices plotted as a function of the time of the K<sub>p</sub> measurement, using 15-day data samples for F3. (Continued)

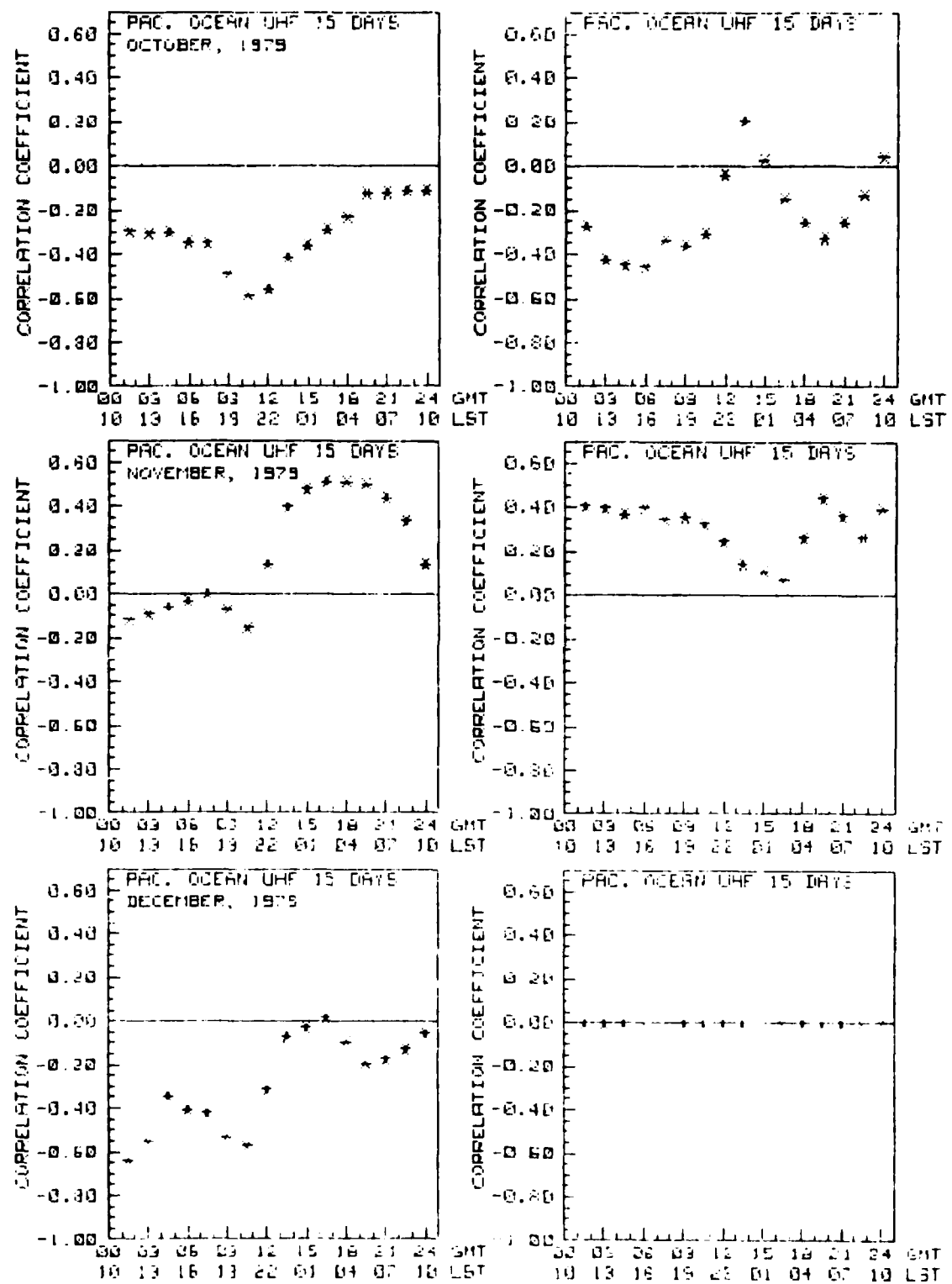


Figure 12. Cross correlations between total hours per night that scintillation fading exceeded 6 dB and the 3-hour K<sub>p</sub> indices plotted as a function of the time of the K<sub>p</sub> measurement, using 15-day data samples for F3. (Continued)

## DISCUSSION

When good correlation, either positive or negative, is obtained between two variables, a cause-and-effect relationship may sometimes be assigned to them. It is not always true, however, that one of them is affecting the other. Sometimes a third factor is affecting them both. It is proposed here that it is not magnetic activity which is affecting the occurrence and intensity of equatorial scintillation but, rather, the solar radiations that are producing the magnetic disturbances which also affect the scintillation. It is further proposed that this can be either a positive effect or a negative effect, depending on when, with respect to the equatorial site, the radiation reaches the earth.

In an earlier report (ref 7), this writer proposed that zonal winds resulting from day-to-night temperature and pressure differences were the generating mechanism which produced the ionospheric irregularities which cause equatorial scintillation. More recently (ref 2), a periodicity was observed in the scintillation data which was attributed to the moon's gravitational attraction increasing or decreasing the zonal winds, depending on the moon's location with respect to the sun.

If zonal winds are indeed the mechanism generating the ionospheric irregularities which cause equatorial scintillation, then a connection between magnetic activity (or, rather, the ionized solar radiations which cause magnetic activity) and the occurrence of scintillation can be made.

Using satellite drag measurements, Jacchia et al (ref 8) found that the temperature and density of the upper atmosphere increased during magnetic storms. Even the smallest variations in geomagnetic activity were reflected in atmospheric variations. They found the temperature changes to be nearly linear with the 3-hour K<sub>p</sub> magnetic index for values of K<sub>p</sub> less than 5. The variation was about 28 degrees/K<sub>p</sub>. For larger K<sub>p</sub>, they found the temperature to vary more linearly with the 3-hour A<sub>p</sub> index (ref 1) at a rate of about 1 degree/A<sub>p</sub>. Temperature changes for latitudes around 25 degrees lagged the magnetic disturbances, with an average time delay of  $7.2 \pm 0.3$  hours.

Perigee heights of the satellites used in the study ranged from 250 to 545 kilometers.

Ionized solar gas, arriving from the sun, propagates down the magnetic field lines to the auroral region, setting up currents which disturb the magnetic field (ref 1). The associated energy raises the temperature and pressure of the thermosphere in the auroral regions. Jones and Rishbeth (ref 9) say that the normal meridional winds at thermospheric heights blow toward the equator on the night side of the earth and toward the poles on the day side. They say that the increased pressure in the polar regions, which arises from the thermospheric heating, increases the equatorward winds at night and decreases the daytime poleward winds.

It is argued here that the heating in the auroral regions by the ionized solar gas can increase or decrease the occurrence and intensity of scintillation at a given equatorial site, depending on when, with respect to the equatorial site, the radiations reach the auroral regions. If they arrive at such time that the energy transmitted by meridional winds raises

7. NOSC TR 290, Zonal Winds as a Generating Mechanism for the Ionospheric Irregularities that Cause Equatorial Scintillation of Satellite Signals, by M.R. Paulson, 26 June 1978.
8. Jacchia, L.G., J. Slowey, and F. Verniani, Geomagnetic Perturbations and Upper Atmosphere Heating, *Journal of Geophysical Research*, v 72, no 5, pp 1423 - 1434, March 1967.
9. Jones, K.L., and H. Rishbeth, The Origin of Storm Increases of Mid-Latitude E-Layer Electron Concentration, *Journal of Atmospheric and Terrestrial Physics*, v 33, pp 391 - 401, 1971.

the nighttime temperature and density of the thermosphere at the equatorial site, the resulting decrease in day-to-night pressure differences will reduce or inhibit the zonal winds and consequently the occurrence and intensity of equatorial scintillation. If they arrive at such time as to increase the daytime temperature and density of the thermosphere, by reducing the poleward meridional winds, the increased day-to-night pressure difference would tend to increase the zonal winds and the occurrence and intensity of the equatorial scintillation.

The positive effects of the solar radiations would be most apparent during times when scintillation occurrence and intensity are quite low. Radiation arriving at times which would normally reduce scintillation would have the same effect, but there would be no scintillation to reduce. On the other hand, radiation arriving at a time so as to increase scintillation could increase the day-to-night pressure differences and produce zonal winds of sufficient velocity, at times, to produce scintillation. During periods of high scintillation activity, the inhibiting nature of the solar radiations would be more apparent since positive contributions would be obscured by the already extensive scintillation activity. During times of moderate scintillation, correlations could be quite low since the effects of radiations arriving at different times of day tend to oppose each other.

## RESULTS

Cross correlations between total daily hours of scintillation with fades greater than 6 dB and the daily summed geomagnetic K<sub>p</sub> indices calculated through the use of 30-day data samples, showed correlations near zero in January which then went rapidly negative in February. Correlations for the Pacific Ocean satellite, F3, stayed negative through most of June, then approached zero for a while before going negative again in September. Correlations for the Indian Ocean satellite, F2, approached zero around mid-May through mid-August before going negative again in September. The correlations were somewhat positive in November and December for both satellites.

Calculations of correlations between the individual 3-hour K<sub>p</sub> indices and the total nightly occurrence of scintillation gave plots of correlation versus time of magnetic activity that showed negative peaks at times, particularly in March and April and again in September. These peaks occurred around 1300 - 1600 LST. In November, a positive maximum occurred around 0200 - 0700 LST.

When only the occurrence of scintillation from 0200 LST and later was used, the cross-correlation plots showed positive correlations for July and August and for October through December. Some of the curves showed positive and negative correlations with magnetic activity for different times of the day.

It is proposed here that it is the ionized solar radiations, which cause the magnetic disturbances, that also affect the occurrence and intensity of equatorial scintillation, and not the magnetic disturbances themselves. It is further proposed that the solar radiations heat the thermosphere in the auroral regions, and that this energy can then increase the temperature and density of the thermosphere in the equatorial regions, either by increasing the equatorward flow of the meridional winds at night or by reducing the poleward flow of the winds in the daytime. It is argued that this temperature and density increase can either increase or decrease the occurrence and intensity of equatorial scintillation, depending on when the temperature and density increase occurs. If it occurs at night, it will tend to reduce or inhibit the scintillation by decreasing the day-to-night temperature and pressure differences, and thus decrease the zonal winds. If it occurs in the daytime, it will tend to increase these differences and thus increase the zonal winds. These variations in zonal wind would show up as variations in the occurrence and intensity of the equatorial scintillation.

## RECOMMENDATIONS

The possible connection between magnetic activity, or ionized solar radiation, and equatorial scintillation needs further investigation. In particular, the part that zonal and meridional winds may play in connecting the two, as well as the part they play in connecting other solar and geophysical phenomena to the occurrence and intensity of scintillation, needs to be investigated.

It is recommended that spaced receivers be used to monitor signals from a satellite for approximately 1 year. The apparent ionospheric drift velocity calculated from the spaced receivers could be used as an indication of the zonal winds. The occurrence and intensity of scintillation, magnetic activity, phases of the moon, and solar activity could be related to this drift velocity, as well as to each other.

Obtaining a continuous measure of meridional winds would probably be quite difficult. For one thing, such measurements should probably be made at midlatitudes at a longitude near that of the equatorial scintillation measurement site. It is not clear at this time how such measurements might be made.

## REFERENCES

1. National Bureau of Standards Monograph 80, Ionospheric Radio Propagation, by K. Davies, U. S. Government Printing Office, 1965.
2. Naval Ocean Systems Center TR 543, Equatorial Scintillation of Satellite Signals at UHF and L-Band for Two Different Elevation Angles, by M.R. Paulson, in progress.
3. Koster, J.P., Equatorial Scintillation, Planetary Space Science, v 20, pp 1999 - 2014, 1972.
4. Bandyopadhyay, P., and J. Aarons, The Equatorial F-Layer Irregularity Extent as Observed from Huancayo, Peru, Radio Science, v 5, no 6, pp 931 - 938, June 1970.
5. Mullen, J.P., Sensitivity of Equatorial Scintillation to Magnetic Activity, Journal of Atmospheric and Terrestrial Physics, v 35, pp 1187 - 1194, 1973.
6. National Oceanic and Atmospheric Administration Environmental Data and Information Service, Solar-Geophysical Data, Prompt Reports, Boulder, CO.
7. NOSC TR 290, Zonal Winds as a Generating Mechanism for the Ionospheric Irregularities that Cause Equatorial Scintillation of Satellite Signals, by M.R. Paulson, 26 June 1978.
8. Jacchia, L.G., J. Slowey, and F. Verniani, Geomagnetic Perturbations and Upper Atmosphere Heating, Journal of Geophysical Research, v 72, no 5, pp 1423 - 1434, March 1967.
9. Jones, K.L., and H. Rishbeth, The Origin of Storm Increases of Mid-Latitude F-Layer Electron Concentration, Journal of Atmospheric and Terrestrial Physics, v 33, pp 391 - 401, 1971.

## APPENDIX

- Table I. Cross-correlation values for figure 3.
- Table II. Cross-correlation values for figure 4.
- Table III. Cross-correlation values for figure 5.
- Table IV. Cross-correlation values for figure 6.
- Table V. Cross-correlation values for figure 7.
- Table VI. Cross-correlation values for figure 8.
- Table VII. Cross-correlation values for figure 9.
- Table VIII. Cross-correlation values for figure 10.
- Table IX. Cross-correlation values for figure 11.
- Table X. Cross-correlation values for figure 12.

PRECEDING PAGE BLANK-NOT FILMED

Table I. Cross-correlation values for figure 3.

INDIAN OCEAN UHF 1979

Kp	1	2	3	4				
JAN.	0.154	0.095	0.024	0.048	0.076	0.174	0.234	0.145
	-0.235	-0.332	-0.411	-0.409	-0.344	-0.328	-0.266	-0.346
FEB.	-0.571	-0.656	-0.627	-0.602	-0.520	-0.604	-0.659	-0.687
	-0.476	-0.485	-0.376	-0.379	-0.339	-0.489	-0.589	-0.592
MAR.	-0.311	-0.305	-0.268	-0.286	-0.408	-0.434	-0.414	-0.312
	-0.389	-0.435	-0.472	-0.604	-0.582	-0.557	-0.479	-0.391
APR.	-0.572	-0.610	-0.618	-0.651	-0.632	-0.627	-0.582	-0.551
	-0.376	-0.412	-0.426	-0.474	-0.492	-0.510	-0.432	-0.485
MAY	0.070	0.019	-0.031	-0.028	-0.141	-0.321	-0.451	-0.380
	0.032	-0.027	-0.079	-0.112	-0.140	-0.287	-0.377	-0.297
JUNE	-0.146	-0.192	-0.210	-0.197	-0.166	-0.260	-0.299	-0.115
	-0.176	-0.164	-0.129	-0.192	-0.231	-0.315	-0.338	-0.213
JULY	0.031	0.066	0.100	-0.142	-0.366	-0.311	-0.204	-0.166
	0.045	0.004	-0.055	-0.158	-0.268	-0.056	0.061	0.209
AUG.	-0.442	-0.542	-0.584	-0.511	-0.389	-0.272	-0.138	0.033
	-0.466	-0.506	-0.472	-0.562	-0.563	-0.511	-0.408	-0.374
SEP.	-0.475	-0.542	-0.512	-0.651	-0.660	-0.555	-0.358	-0.329
	-0.232	-0.242	-0.228	-0.419	-0.551	-0.532	-0.445	-0.325
OCT.	-0.010	-0.020	-0.030	-0.059	-0.073	-0.173	-0.250	-0.074
	-0.328	-0.333	-0.301	-0.260	-0.153	-0.272	-0.360	-0.149
NOV.	-0.147	-0.099	-0.048	-0.044	-0.030	-0.038	-0.040	0.126
	-0.170	-0.172	-0.152	-0.066	0.037	0.023	0.002	0.055
DEC.	0.067	-0.025	-0.109	-0.010	0.103	-0.032	-0.157	-0.100
Kp	5	6	7	8				
JAN.	0.051	0.044	0.034	0.077	0.105	0.081	0.045	0.070
	-0.376	-0.324	-0.242	-0.255	-0.227	-0.263	-0.271	-0.186
FEB.	-0.652	-0.628	-0.537	-0.567	-0.537	-0.506	-0.432	-0.461
	-0.554	-0.502	-0.402	-0.417	-0.387	-0.362	-0.321	-0.447
MAR.	-0.192	-0.197	-0.191	-0.312	-0.283	-0.344	-0.348	-0.414
	-0.276	-0.300	-0.287	-0.264	-0.307	-0.366	-0.327	-0.322
APR.	-0.492	-0.465	-0.363	-0.415	-0.427	-0.423	-0.382	-0.421
	-0.442	-0.417	-0.339	-0.389	-0.408	-0.371	-0.310	-0.324
MAY	-0.265	-0.279	-0.266	-0.311	-0.275	-0.205	-0.135	-0.111
	-0.180	-0.216	-0.216	-0.262	-0.211	-0.273	-0.214	-0.158
JUNE	0.039	0.010	-0.018	-0.078	-0.114	-0.153	-0.180	-0.101
	-0.069	-0.004	0.058	-0.009	-0.074	-0.152	-0.232	-0.185
JULY	-0.109	-0.141	-0.155	-0.307	-0.275	-0.215	-0.027	-0.055
	0.334	0.260	0.147	0.095	0.036	0.096	0.141	0.076
AUG.	0.192	0.117	0.034	0.072	0.106	0.110	0.095	0.001
	-0.308	-0.293	-0.242	-0.168	-0.072	-0.055	-0.023	-0.045
SEP.	-0.256	-0.282	-0.274	-0.325	-0.273	-0.132	0.052	0.121
	-0.126	-0.192	-0.242	-0.266	-0.217	-0.044	0.114	0.107
OCT.	0.109	0.054	-0.006	0.102	0.211	0.185	0.136	0.067
	0.081	0.085	0.079	0.124	0.164	0.185	0.184	0.016
NOV.	0.262	0.307	0.310	0.324	0.339	0.364	0.366	0.207
	0.108	0.118	0.115	0.179	0.229	0.266	0.274	0.174
DEC.	-0.026	-0.005	0.016	-0.001	-0.020	0.029	0.071	0.126

Table II. Cross-correlation values for figure 4.

## PACIFIC OCEAN UHF 1979

Kp	1	2	3	4				
JAN.	-0.101	-0.049	0.009	0.042	0.085	0.163	0.203	0.132
	-0.235	-0.316	-0.379	-0.372	-0.305	-0.303	-0.266	-0.367
FEB.	-0.457	-0.477	-0.414	-0.427	-0.398	-0.446	-0.463	-0.524
	-0.459	-0.468	-0.363	-0.376	-0.345	-0.460	-0.417	-0.461
MAR.	-0.537	-0.571	-0.557	-0.533	-0.377	-0.314	-0.227	-0.180
	-0.569	-0.649	-0.720	-0.705	-0.499	-0.411	-0.293	-0.263
APR.	-0.641	-0.708	-0.743	-0.724	-0.643	-0.628	-0.573	-0.579
	-0.494	-0.537	-0.550	-0.565	-0.540	-0.527	-0.492	-0.427
MAY	-0.142	-0.254	-0.334	-0.389	-0.393	-0.397	-0.332	-0.271
	-0.331	-0.419	-0.474	-0.503	-0.491	-0.492	-0.377	-0.345
JUNE	-0.588	-0.536	-0.422	-0.450	-0.437	-0.512	-0.443	-0.271
	-0.382	-0.288	-0.151	-0.178	-0.166	-0.181	-0.161	-0.079
JULY	-0.037	0.036	0.131	0.092	0.027	0.174	0.261	0.280
	-0.042	-0.053	-0.058	-0.174	-0.231	-0.040	0.102	0.127
AUG.	-0.333	-0.351	-0.326	-0.376	-0.396	-0.349	-0.259	-0.192
	-0.305	-0.283	-0.229	-0.293	-0.312	-0.319	-0.290	-0.221
SEP.	-0.506	-0.541	-0.483	-0.560	-0.528	-0.423	-0.247	-0.178
	-0.498	-0.532	-0.513	-0.622	-0.639	-0.589	-0.463	-0.393
OCT.	-0.167	-0.236	-0.283	-0.293	-0.249	-0.293	-0.303	-0.210
	-0.194	-0.200	-0.183	-0.171	-0.117	-0.244	-0.348	-0.130
NOV.	0.064	0.097	0.122	0.138	0.129	0.104	0.057	0.206
	0.376	0.325	0.241	0.280	0.272	0.296	0.284	0.207
DEC.	0.140	0.161	0.155	0.130	0.092	0.026	-0.640	-0.014
Kp	5	6	7	8				
JAN.	0.055	-0.039	-0.110	-0.053	0.000	-0.165	-0.127	-0.115
	-0.418	-0.415	-0.347	-0.391	-0.371	-0.337	-0.269	-0.193
FEB.	-0.528	-0.543	-0.496	-0.519	-0.487	-0.440	-0.354	-0.357
	-0.471	-0.500	-0.483	-0.494	-0.452	-0.387	-0.310	-0.414
MAR.	-0.121	-0.153	-0.175	-0.261	-0.238	-0.298	-0.143	-0.406
	-0.216	-0.154	-0.075	-0.206	-0.197	-0.209	-0.116	-0.149
APR.	-0.554	-0.493	-0.147	-0.322	-0.268	-0.181	-0.035	-0.125
	-0.332	-0.375	-0.385	-0.475	-0.524	-0.458	-0.366	-0.333
MAY	-0.179	-0.215	-0.232	-0.180	-0.094	-0.088	-0.078	-0.043
	-0.279	-0.348	-0.337	-0.314	-0.193	-0.167	-0.122	-0.111
JUNE	-0.099	-0.166	-0.215	-0.230	-0.203	-0.158	-0.084	-0.071
	0.032	-0.005	-0.013	-0.035	-0.048	-0.047	-0.039	-0.011
JULY	0.260	0.165	0.055	-0.001	-0.053	-0.002	0.051	-0.012
	0.142	0.054	-0.059	-0.077	-0.084	0.017	0.163	0.074
AUG.	-0.112	-0.063	-0.011	-0.002	0.007	0.100	0.183	0.108
	-0.131	-0.056	0.006	0.024	0.041	0.083	0.117	0.070
SEP.	-0.086	-0.175	-0.252	-0.314	-0.278	-0.131	0.057	0.099
	-0.232	-0.291	-0.326	-0.413	-0.404	-0.106	0.016	0.067
OCT.	-0.079	-0.087	-0.086	-0.026	0.042	0.021	-0.002	0.044
	0.105	0.141	0.154	0.196	0.226	0.201	0.142	0.025
NOV.	0.337	0.397	0.424	0.477	0.503	0.434	0.329	0.236
	0.112	0.085	0.050	0.185	0.222	0.289	0.270	0.151
DEC.	0.016	0.012	0.004	-0.005	-0.015	0.151	0.272	0.254

Table III. Cross-correlation values for figure 5.

INDIAN OCEAN UHF 1979

Kp	1	2	3	4				
MAR.	-0.420	-0.399	-0.334	-0.467	-0.482	-0.494	-0.457	-0.367
	-0.436	-0.493	-0.542	-0.685	-0.654	-0.619	-0.526	-0.445
APR.	-0.571	-0.623	-0.647	-0.684	-0.687	-0.655	-0.601	-0.578
	-0.255	-0.412	-0.445	-0.500	-0.523	-0.542	-0.524	-0.506
MAY	0.009	-0.068	-0.130	-0.211	-0.269	-0.452	-0.563	-0.403
	0.085	0.026	-0.023	-0.061	-0.100	-0.312	-0.466	-0.366
JUNE	-0.080	-0.099	-0.103	-0.078	-0.046	-0.246	-0.430	-0.215
	-0.322	-0.320	-0.264	-0.298	-0.289	-0.384	-0.402	-0.257
JULY	0.002	0.040	0.087	-0.157	-0.370	-0.320	-0.216	-0.183
	0.029	-0.016	-0.075	-0.191	-0.243	-0.116	-0.610	0.085
AUG.	-0.354	-0.444	-0.430	-0.438	-0.442	-0.420	-0.338	-0.199
	-0.350	-0.372	-0.354	-0.510	-0.591	-0.613	-0.566	-0.522
SEP.	-0.465	-0.534	-0.507	-0.666	-0.682	-0.586	-0.584	-0.333
	-0.356	-0.370	-0.347	-0.506	-0.593	-0.587	-0.507	-0.365
OCT.	-0.222	-0.254	-0.259	-0.238	-0.172	-0.282	-0.362	-0.202
	-0.423	-0.431	-0.392	-0.318	-0.161	-0.265	-0.392	-0.177
NOV.	-0.185	-0.141	-0.093	-0.095	-0.078	-0.063	-0.036	0.082
Kp	5	6	7	8				
MAR.	-0.256	-0.252	-0.235	-0.314	-0.274	-0.321	-0.292	-0.366
	-0.394	-0.329	-0.303	-0.370	-0.369	-0.357	-0.288	-0.283
APR.	-0.525	-0.472	-0.337	-0.385	-0.386	-0.381	-0.213	-0.361
	-0.450	-0.412	-0.318	-0.368	-0.387	-0.355	-0.300	-0.301
MAY	-0.346	-0.365	-0.349	-0.368	-0.323	-0.223	-0.173	-0.115
	-0.231	-0.236	-0.225	-0.282	-0.285	-0.273	-0.234	-0.133
JUNE	-0.021	-0.014	-0.007	-0.127	-0.205	-0.240	-0.253	-0.140
	-0.087	-0.024	0.007	-0.016	-0.065	-0.116	-0.170	-0.124
JULY	-0.129	-0.156	-0.165	-0.322	-0.392	-0.261	-0.097	-0.122
	0.167	0.081	-0.030	-0.085	-0.123	-0.051	0.022	-0.057
AUG.	-0.049	-0.098	-0.128	-0.095	-0.052	-0.053	-0.044	-0.120
	-0.433	-0.406	-0.320	-0.265	-0.175	-0.210	-0.203	-0.137
SEP.	-0.241	-0.295	-0.316	-0.350	-0.267	-0.154	0.008	0.072
	-0.135	-0.158	-0.160	-0.238	-0.253	-0.013	0.196	0.251
OCT.	-0.009	-0.004	0.001	0.044	0.087	0.125	0.145	0.166
	0.007	0.023	0.032	0.074	0.112	0.137	0.147	0.033
NOV.	0.193	0.234	0.253	0.282	0.295	0.327	0.398	0.226

Table IV. Cross-correlation values for figure 6.

## PACIFIC OCEAN UHF 1979

Kp	1	2	3	4				
MAR.	-0.518	-0.557	-0.553	-0.551	-0.413	-0.356	-0.271	-0.212
	-0.572	-0.646	-0.711	-0.736	-0.563	-0.496	-0.296	-0.357
APR.	-0.625	-0.699	-0.742	-0.730	-0.655	-0.635	-0.574	-0.582
	-0.455	-0.516	-0.587	-0.563	-0.550	-0.540	-0.486	-0.455
MAY	-0.160	-0.273	-0.353	-0.395	-0.385	-0.374	-0.296	-0.247
	-0.162	-0.241	-0.299	-0.321	-0.317	-0.312	-0.292	-0.194
JUNE	-0.379	-0.295	-0.183	-0.222	-0.241	-0.305	-0.251	-0.082
	-0.387	-0.307	-0.182	-0.181	-0.152	-0.127	-0.076	0.022
JULY	-0.032	0.039	0.133	0.094	0.029	0.198	0.298	0.324
	-0.064	-0.047	-0.014	-0.146	-0.228	-0.094	0.017	0.038
AUG.	-0.297	-0.305	-0.275	-0.347	-0.390	-0.391	-0.331	-0.288
	-0.248	-0.230	-0.194	-0.305	-0.372	-0.383	-0.351	-0.277
SEP.	-0.462	-0.427	-0.326	-0.455	-0.493	-0.418	-0.274	-0.294
	-0.513	-0.466	-0.368	-0.495	-0.532	-0.528	-0.458	-0.447
OCT.	-0.246	-0.300	-0.323	-0.325	-0.266	-0.334	-0.364	-0.233
	-0.259	-0.245	-0.203	-0.206	-0.162	-0.271	-0.348	-0.177
NOV.	0.016	0.042	0.063	0.052	0.026	0.021	0.009	0.096
Kp	5	6	7	8				
MAR.	-0.141	-0.180	-0.209	-0.268	-0.132	-0.285	-0.296	-0.366
	-0.304	-0.236	-0.140	-0.233	-0.208	-0.218	-0.113	-0.170
APR.	-0.559	-0.489	-0.331	-0.309	-0.258	-0.169	-0.061	-0.128
	-0.391	-0.419	-0.406	-0.474	-0.582	-0.454	-0.377	-0.342
MAY	-0.169	-0.206	-0.213	-0.136	-0.093	-0.054	-0.064	-0.032
	-0.136	-0.201	-0.247	-0.124	-0.018	-0.015	-0.012	0.016
JUNE	0.085	0.058	0.013	0.012	0.008	0.048	0.092	0.108
	0.036	0.091	0.079	0.059	0.023	0.042	0.061	0.073
JULY	0.305	0.162	0.004	-0.048	-0.036	0.001	0.088	-0.016
	0.055	-0.057	-0.188	-0.181	-0.150	-0.043	0.061	-0.045
AUG.	-0.223	-0.165	-0.091	-0.093	-0.027	-0.017	0.061	-0.034
	-0.178	-0.123	-0.064	-0.076	-0.091	-0.057	-0.017	-0.079
SEP.	-0.286	-0.388	-0.438	-0.460	-0.327	-0.268	-0.131	-0.126
	-0.334	-0.387	-0.406	-0.464	-0.396	-0.231	-0.047	0.006
OCT.	-0.062	-0.070	-0.070	-0.039	0.005	0.011	0.016	0.085
	0.016	0.054	0.078	0.132	0.172	0.158	0.112	0.018
NOV.	0.175	0.253	0.303	0.364	0.405	0.321	0.208	0.184

Table V. Cross-correlation values for figure 7.

## INDIAN OCEAN L-BAND 1979

Kp	1	2	3	4				
	5	6	7	8				
MAR.	-0.251 -0.268	-0.178 -0.253	-0.066 -0.300	-0.309 -0.506	-0.471 -0.591	-0.507 -0.574	-0.490 -0.561	-0.441 -0.466
APR.	-0.515 -0.272	-0.560 -0.295	-0.578 -0.302	-0.622 -0.365	-0.618 -0.406	-0.611 -0.433	-0.565 -0.432	-0.545 -0.439
MAY	-0.015 0.056	-0.040 0.031	-0.059 0.006	-0.147 -0.059	-0.227 -0.127	-0.404 -0.343	-0.516 -0.493	-0.499 -0.432
JUNE	-0.126 -0.510	-0.139 -0.498	-0.133 -0.417	-0.110 -0.439	-0.076 -0.298	-0.015 -0.455	-0.527 -0.422	-0.256 -0.241
JULY	-0.023 -0.001	0.024 -0.003	0.087 -0.005	-0.081 -0.050	-0.234 -0.142	-0.181 -0.068	-0.101 -0.003	-0.079 0.073
AUG.	-0.311 -0.319	-0.367 -0.325	-0.383 -0.295	-0.407 -0.434	-0.397 -0.509	-0.399 -0.505	-0.340 -0.446	-0.229 -0.440
SEP.	-0.501 -0.399	-0.550 -0.432	-0.504 -0.422	-0.611 -0.561	-0.598 -0.619	-0.520 -0.623	-0.358 -0.550	-0.298 -0.393
OCT.	-0.250 -0.410	-0.285 -0.399	-0.289 -0.344	-0.273 -0.253	-0.205 -0.092	-0.301 -0.181	-0.265 -0.251	-0.194 -0.095
NOV.	-0.171	-0.120	-0.065	-0.059	-0.040	-0.017	0.012	0.122
MAR.	-0.365 -0.400	-0.359 -0.347	-0.335 -0.254	-0.332 -0.300	-0.266 -0.246	-0.313 -0.268	-0.287 -0.161	-0.337 -0.149
APR.	-0.496 -0.413	-0.432 -0.366	-0.290 -0.268	-0.364 -0.330	-0.402 -0.363	-0.377 -0.329	-0.322 -0.274	-0.361 -0.285
MAY	-0.418 -0.327	-0.455 -0.328	-0.448 -0.309	-0.397 -0.218	-0.259 -0.268	-0.197 -0.269	-0.128 -0.249	-0.051 -0.151
JUNE	-0.014 -0.047	-0.006 -0.017	0.003 0.013	-0.116 -0.005	-0.195 -0.021	-0.225 -0.061	-0.233 -0.104	-0.130 -0.076
JULY	-0.049 0.139	-0.095 0.045	-0.128 -0.073	-0.222 -0.101	-0.256 -0.112	-0.155 -0.042	-0.034 0.027	-0.088 -0.062
AUG.	-0.103 -0.399	-0.149 -0.382	-0.171 -0.317	-0.157 -0.249	-0.129 -0.153	-0.124 -0.189	-0.098 -0.196	-0.152 -0.173
SEP.	-0.201 -0.142	-0.255 -0.173	-0.281 -0.190	-0.293 -0.292	-0.206 -0.310	-0.142 -0.095	-0.016 0.101	0.011 0.160
OCT.	0.007 0.075	0.016 0.075	0.027 0.069	0.060 0.102	0.099 0.130	0.104 0.105	0.105 0.102	0.147 0.012
NOV.	0.220	0.253	0.265	0.291	0.301	0.319	0.315	0.217

Table VI. Cross-correlation values for figure 8.

## PACIFIC OCEAN UHF FM 1979

Kp	1	2	3	4				
MAR.	-0.549	-0.520	-0.536	-0.521	-0.377	-0.315	-0.230	-0.179
	-0.554	-0.624	-0.684	-0.709	-0.544	-0.466	-0.352	-0.324
APR.	-0.153	-0.623	-0.669	-0.669	-0.613	-0.583	-0.516	-0.524
	-0.387	-0.450	-0.497	-0.528	-0.534	-0.509	-0.442	-0.426
MAY	-0.339	-0.249	-0.316	-0.336	-0.310	-0.267	-0.174	-0.154
	-0.092	-0.134	-0.164	-0.153	-0.126	-0.117	-0.086	-0.071
JUNE	-0.170	-0.240	-0.121	-0.156	-0.177	-0.233	-0.231	0.002
	-0.458	-0.413	-0.309	-0.314	-0.272	-0.209	-0.105	0.036
JULY	-0.234	-0.133	-0.070	-0.169	-0.229	-0.025	0.148	0.132
	-0.138	-0.108	-0.045	-0.238	-0.346	-0.265	-0.160	-0.176
AUG.	-0.406	-0.205	-0.147	-0.228	-0.293	-0.328	-0.306	-0.273
	-0.203	-0.198	-0.171	-0.274	-0.337	-0.334	-0.295	-0.210
SEP.	-0.249	-0.383	-0.300	-0.429	-0.471	-0.424	-0.310	-0.314
	-0.536	-0.492	-0.394	-0.514	-0.559	-0.566	-0.503	-0.515
OCT.	-0.009	-0.303	-0.327	-0.326	-0.265	-0.325	-0.347	-0.244
	-0.251	-0.230	-0.183	-0.182	-0.138	-0.238	-0.311	-0.171
NOV.	0.292	0.019	0.044	0.035	0.017	0.021	0.023	0.035
Kp	5	6	7	8				
MAR.	-0.118	-0.162	-0.198	-0.260	-0.225	-0.266	-0.248	-0.330
	-0.274	-0.221	-0.142	-0.223	-0.197	-0.202	-0.090	-0.151
APR.	-0.523	-0.488	-0.371	-0.323	-0.246	-0.163	-0.082	-0.118
	-0.378	-0.445	-0.474	-0.519	-0.522	-0.487	-0.413	-0.371
MAY	-0.115	-0.160	-0.152	-0.171	-0.112	-0.126	-0.128	-0.132
	-0.055	-0.110	-0.153	-0.076	0.001	0.009	0.016	0.022
JUNE	0.174	0.166	0.144	0.119	0.074	0.122	0.162	0.144
	0.140	0.149	0.143	0.154	0.124	0.138	0.142	0.116
JULY	0.100	-0.027	-0.147	-0.182	-0.170	-0.125	-0.065	-0.139
	-0.178	-0.278	-0.377	-0.291	-0.352	-0.285	-0.193	-0.278
AUG.	-0.218	-0.169	-0.100	-0.137	-0.161	-0.068	0.042	-0.041
	-0.105	-0.162	-0.086	-0.105	-0.110	-0.046	0.039	-0.040
SEP.	-0.280	-0.383	-0.443	-0.474	-0.346	-0.275	-0.123	-0.124
	-0.412	-0.452	-0.453	-0.513	-0.434	-0.282	-0.101	-0.041
OCT.	-0.098	-0.093	-0.078	-0.040	0.011	0.006	0.001	0.061
	-0.009	0.044	0.079	0.143	0.200	0.164	0.101	0.009
NOV.	0.158	0.237	0.261	0.354	0.400	0.306	0.183	0.155

Table VII. Cross-correlation values for figure 9.

## PACIFIC OCEAN UHF AM 1979

Ep	1	2	3	4				
MAR.	-0.598	-0.603	-0.550	-0.591	-0.466	-0.426	-0.348	-0.274
	-0.545	-0.622	-0.690	-0.712	-0.543	-0.502	-0.415	-0.387
APR.	-0.619	-0.700	-0.730	-0.697	-0.603	-0.604	-0.567	-0.555
	-0.500	-0.534	-0.538	-0.535	-0.493	-0.508	-0.487	-0.435
MAY	-0.119	-0.228	-0.308	-0.365	-0.376	-0.402	-0.359	-0.290
	-0.188	-0.292	-0.371	-0.425	-0.449	-0.443	-0.301	-0.273
JUNE	-0.333	-0.293	-0.219	-0.254	-0.266	-0.325	-0.296	-0.177
	-0.173	-0.074	0.040	0.049	0.050	0.020	-0.014	-0.002
JULY	0.137	0.224	0.320	0.365	0.315	0.386	0.368	0.434
	0.042	0.039	0.027	0.002	-0.021	0.136	0.222	0.280
AUG.	-0.307	-0.369	-0.392	-0.427	-0.426	-0.372	-0.272	-0.227
	-0.250	-0.231	-0.188	-0.286	-0.342	-0.376	-0.366	-0.332
SEP.	-0.491	-0.440	-0.322	-0.430	-0.452	-0.326	-0.160	-0.207
	-0.411	-0.363	-0.275	-0.374	-0.419	-0.394	-0.318	-0.255
OCT.	-0.289	-0.256	-0.276	-0.282	-0.236	-0.215	-0.359	-0.179
	-0.252	-0.250	-0.221	-0.231	-0.190	-0.304	-0.361	-0.173
NOV.	0.062	0.082	0.096	0.080	0.045	0.019	-0.016	0.095
Ep	5	6	7	8				
MAR.	-0.184	-0.206	-0.218	-0.268	-0.229	-0.307	-0.389	-0.488
	-0.334	-0.240	-0.119	-0.227	-0.207	-0.227	-0.147	-0.192
APR.	-0.514	-0.395	-0.195	-0.224	-0.231	-0.146	-0.064	-0.121
	-0.352	-0.311	-0.225	-0.323	-0.391	-0.325	-0.249	-0.240
MAY	-0.186	-0.189	-0.170	-0.041	0.079	0.062	0.043	0.099
	-0.189	-0.242	-0.275	-0.151	-0.022	-0.028	-0.031	0.015
JUNE	-0.060	-0.120	-0.170	-0.140	-0.091	-0.067	-0.030	0.029
	0.008	-0.012	-0.030	-0.083	-0.113	-0.095	-0.062	-0.007
JULY	0.436	0.323	0.176	0.122	0.340	0.145	0.225	0.120
	0.314	0.222	0.092	0.122	0.114	0.256	0.343	0.244
AUG.	-0.164	-0.110	-0.047	0.002	0.053	0.068	0.073	-0.013
	-0.170	-0.136	-0.006	-0.001	0.004	-0.057	-0.118	-0.130
SEP.	-0.291	-0.111	-0.356	-0.352	-0.237	-0.210	-0.123	-0.109
	-0.134	-0.208	-0.265	-0.111	-0.274	-0.099	0.071	0.108
OCT.	0.028	-0.003	-0.043	-0.010	-0.010	0.021	0.049	0.129
	0.056	0.063	0.070	0.102	0.129	0.134	0.121	0.032
NOV.	0.193	0.271	0.315	0.364	0.394	0.312	0.242	0.171

Table VIII. Cross-correlation values for figure 10.

## PAC. OCEAN UHF TO 2 FM 1979

Kp	1	2	3	4				
					5	6	7	8
JAN.	-0.054 -0.216	-0.012 -0.290	0.031 -0.347	0.062 -0.350	0.100 -0.301	0.150 -0.264	0.165 -0.184	0.103 -0.327
FEB.	-0.453 -0.410	-0.458 -0.426	-0.393 -0.339	-0.404 -0.346	-0.305 -0.302	-0.415 -0.350	-0.419 -0.365	-0.494 -0.411
MAR.	-0.512 -0.585	-0.564 -0.666	-0.574 -0.727	-0.507 -0.707	-0.315 -0.484	-0.232 -0.390	-0.136 -0.268	-0.079 -0.234
APR.	-0.615 -0.479	-0.606 -0.528	-0.726 -0.547	-0.716 -0.579	-0.646 -0.572	-0.631 -0.561	-0.577 -0.506	-0.593 -0.461
MAY	-0.196 -0.330	-0.268 -0.409	-0.357 -0.457	-0.407 -0.465	-0.404 -0.473	-0.397 -0.450	-0.318 -0.319	-0.268 -0.312
JUNE	-0.600 -0.466	-0.541 -0.384	-0.419 -0.245	-0.470 -0.260	-0.478 -0.237	-0.523 -0.196	-0.410 -0.117	-0.264 -0.045
JULY	-0.149 -0.119	-0.091 -0.103	-0.064 -0.061	-0.036 -0.221	-0.060 -0.304	0.121 -0.187	0.246 -0.071	0.263 -0.054
AUG.	-0.290 -0.275	-0.302 -0.283	-0.276 -0.261	-0.361 -0.335	-0.417 -0.357	-0.436 -0.385	-0.384 -0.368	-0.336 -0.311
SEP.	-0.526 -0.517	-0.544 -0.527	-0.470 -0.483	-0.551 -0.600	-0.525 -0.629	-0.434 -0.602	-0.270 -0.499	-0.234 -0.465
OCT.	-0.200 -0.244	-0.272 -0.242	-0.319 -0.214	-0.322 -0.220	-0.267 -0.175	-0.335 -0.270	-0.365 -0.330	-0.286 -0.180
NOV.	0.019 0.287	0.043 0.196	0.063 0.097	0.057 0.116	0.039 0.115	0.036 0.094	0.026 0.055	0.095 0.035
DEC.	0.140	0.161	0.155	0.130	0.092	0.026	-0.040	-0.014
	Kp	5	6	7	8			
JAN.	0.036 -0.416	-0.054 -0.379	-0.122 -0.283	-0.074 -0.322	-0.027 -0.307	-0.092 -0.265	-0.149 -0.194	-0.134 -0.175
FEB.	-0.520 -0.428	-0.510 -0.474	-0.445 -0.476	-0.467 -0.460	-0.439 -0.396	-0.391 -0.334	-0.308 -0.261	-0.350 -0.357
MAR.	-0.019 -0.184	-0.063 -0.125	-0.104 -0.053	-0.225 -0.134	-0.213 -0.130	-0.287 -0.203	-0.390 -0.115	-0.349 -0.151
APR.	-0.577 -0.382	-0.517 -0.433	-0.366 -0.445	-0.338 -0.532	-0.281 -0.575	-0.198 -0.514	-0.114 -0.422	-0.151 -0.183
MAY	-0.186 -0.273	-0.247 -0.364	-0.287 -0.422	-0.232 -0.293	-0.190 -0.135	-0.125 -0.116	-0.110 -0.081	-0.097 -0.097
JUNE	-0.113 0.020	-0.161 0.027	-0.153 0.030	-0.157 0.001	-0.168 -0.029	-0.117 -0.013	-0.042 0.006	-0.078 0.007
JULY	0.243 -0.033	0.123 -0.135	-0.008 -0.249	-0.048 -0.256	-0.074 -0.230	-0.056 -0.160	-0.031 -0.078	-0.107 -0.187
AUG.	-0.262 -0.227	-0.216 -0.173	-0.137 -0.108	-0.127 -0.087	-0.107 -0.056	-0.028 -0.017	0.061 0.032	-0.072 -0.027
SEP.	-0.168 -0.326	-0.262 -0.403	-0.338 -0.446	-0.292 -0.518	-0.220 -0.451	-0.167 -0.244	0.028 -0.022	0.068 0.017
OCT.	-0.153 -0.007	-0.175 0.037	-0.178 0.067	-0.098 0.117	0.012 0.162	-0.023 0.131	-0.051 0.078	-0.019 0.009
NOV.	0.155 -0.127	0.232 -0.166	0.282 -0.185	0.349 -0.095	0.397 0.052	0.299 -0.020	0.171 -0.041	0.147 0.062
DEC.	0.018	0.012	0.004	-0.006	-0.015	0.151	0.279	0.324

Table IX. Cross-correlation values for figure 11.

## FAC. OCEAN 2 AM ON 1979

Kp	1	2	3	4				
JAN.	-0.244 -0.075	-0.189 -0.102	-0.110 -0.124	-0.099 -0.097	-0.069 -0.046	0.070 -0.131	0.202 -0.214	0.154 -0.140
FEB.	-0.031 -0.428	-0.081 -0.418	-0.116 -0.302	-0.091 -0.340	-0.058 -0.338	-0.117 -0.390	-0.214 -0.428	-0.140 -0.118
MAR.	-0.349 -0.127	-0.304 -0.157	-0.218 -0.138	-0.350 -0.295	-0.354 -0.330	-0.428 -0.340	-0.406 -0.314	-0.429 -0.423
APR.	-0.454 -0.356	-0.480 -0.360	-0.472 -0.345	-0.419 -0.282	-0.327 -0.195	-0.314 -0.222	-0.282 -0.237	-0.335 -0.234
MAY	0.023 -0.197	-0.068 -0.267	-0.146 -0.316	-0.169 -0.335	-0.211 -0.326	-0.244 -0.384	-0.237 -0.236	-0.119 -0.172
JUNE	-0.233 -0.015	-0.231 0.054	-0.199 0.112	-0.152 0.099	-0.093 0.065	-0.204 -0.055	-0.284 -0.165	-0.140 -0.106
JULY	0.202 0.134	0.271 0.076	0.339 -0.019	0.304 0.017	0.188 0.045	0.197 0.276	0.167 0.389	0.182 0.416
AUG.	-0.283 -0.275	-0.305 -0.171	-0.296 -0.046	-0.249 -0.056	-0.184 -0.056	-0.022 0.001	0.110 0.054	0.187 0.133
SEP.	-0.246 -0.199	-0.325 -0.277	-0.342 -0.331	-0.373 -0.365	-0.334 -0.343	-0.225 -0.259	-0.074 -0.128	0.076 -0.008
OCT.	-0.023 -0.059	-0.055 -0.075	-0.084 -0.084	-0.107 -0.042	-0.111 0.015	-0.077 -0.138	-0.031 -0.294	0.063 -0.006
NOV.	0.106 0.258	0.140 0.299	0.163 0.295	0.205 0.339	0.212 0.324	0.164 0.400	0.081 0.437	0.292 0.430
DEC.	0.140	0.161	0.155	0.130	0.092	0.026	-0.040	-0.014
Kp	5	6	7	8				
JAN.	0.096 -0.655	0.077 -0.140	0.055 -0.194	0.104 -0.213	0.136 -0.198	0.130 -0.216	0.108 -0.312	0.098 -0.067
FEB.	-0.049 -0.422	-0.127 -0.401	-0.184 -0.542	-0.108 -0.415	-0.173 -0.441	-0.175 -0.391	-0.163 -0.326	-0.037 -0.415
MAR.	-0.403 -0.334	-0.373 -0.284	-0.324 -0.199	-0.249 -0.181	-0.180 -0.138	-0.251 -0.142	-0.342 -0.062	-0.390 -0.052
APR.	-0.176 0.003	-0.146 0.007	-0.089 0.011	-0.087 -0.052	-0.079 -0.107	-0.012 -0.048	0.042 0.007	0.065 0.026
MAY	-0.031 -0.173	-0.049 -0.166	-0.001 -0.145	0.022 -0.230	0.036 -0.259	0.040 -0.213	0.046 -0.149	0.086 -0.098
JUNE	-0.010 -0.036	-0.082 -0.062	-0.153 -0.091	-0.185 -0.090	-0.181 -0.064	-0.173 -0.090	-0.143 -0.113	-0.019 -0.058
JULY	0.171 0.409	0.172 0.399	0.154 0.352	0.094 0.322	0.014 0.254	0.167 0.360	0.189 0.421	0.183 0.454
AUG.	0.245 0.205	0.269 0.306	0.256 0.340	0.259 0.342	0.242 0.210	0.325 0.348	0.356 0.322	0.356 0.329
SEP.	0.219 0.123	0.185 0.146	0.129 0.151	0.067 0.047	-0.030 -0.095	0.040 0.013	0.100 0.105	0.164 0.163
OCT.	0.141 0.276	0.170 0.290	0.180 0.270	0.157 0.266	0.102 0.188	0.125 0.273	0.129 0.213	0.188 0.048
NOV.	0.477 0.394	0.432 0.402	0.477 0.367	0.491 0.465	0.478 0.511	0.474 0.563	0.437 0.556	0.290 0.546
DEC.	0.016	0.012	0.004	-0.006	-0.015	0.151	0.279	0.334

Table X. Cross-correlation values for figure 12.

## FAC. OCEAN UHF 15-DAY 1979

Kp	1	2	3	4				
JAN.	-0.325	-0.229	-0.094	-0.060	-0.051	0.156	0.317	0.203
	-0.149	-0.105	-0.051	0.005	0.091	0.147	0.176	0.096
FEB.	-0.114	-0.284	-0.417	-0.408	-0.385	-0.273	-0.182	-0.248
	-0.679	-0.664	-0.446	-0.479	-0.467	-0.590	-0.571	-0.754
MAR.	-0.360	-0.368	-0.247	-0.261	-0.231	-0.254	-0.255	-0.262
	-0.674	-0.735	-0.788	-0.773	-0.523	-0.320	-0.209	-0.119
APR.	-0.504	-0.612	-0.703	-0.640	-0.462	-0.439	-0.391	-0.408
	-0.781	-0.810	-0.809	-0.822	-0.613	-0.802	-0.751	-0.731
MAY	-0.242	-0.309	-0.313	-0.322	-0.293	-0.268	-0.360	-0.193
	-0.244	-0.403	-0.520	-0.585	-0.530	-0.536	-0.414	-0.429
JUNE	-0.548	-0.523	-0.479	-0.467	-0.434	-0.486	-0.347	-0.239
	-0.639	-0.552	-0.343	-0.408	-0.419	-0.531	-0.572	-0.314
JULY	-0.243	-0.134	-0.004	-0.012	-0.019	0.066	0.165	0.153
	0.133	0.205	0.304	0.253	0.109	0.294	0.378	0.432
AUG.	-0.187	-0.323	-0.372	-0.462	-0.503	-0.353	-0.162	-0.149
	-0.390	-0.354	-0.238	-0.304	-0.309	-0.393	-0.327	-0.227
SEP.	-0.068	-0.067	-0.053	-0.172	-0.234	-0.167	-0.074	-0.096
	-0.804	-0.913	-0.887	-0.858	-0.741	-0.615	-0.378	-0.306
OCT.	-0.295	-0.305	-0.301	-0.246	-0.350	-0.492	-0.583	-0.558
	-0.274	-0.426	-0.445	-0.454	-0.335	-0.362	-0.303	-0.039
NOV.	-0.116	-0.089	-0.057	-0.032	0.003	-0.074	-0.151	0.136
	0.407	0.401	0.370	0.397	0.345	0.357	0.329	0.248
DEC.	-0.639	-0.552	-0.243	-0.408	-0.419	-0.531	-0.572	-0.314
Kp	5	6	7	8				
JAN.	0.144	0.100	0.065	0.131	0.181	0.195	0.166	0.162
	-0.022	-0.205	-0.276	-0.131	-0.291	-0.220	-0.214	-0.290
FEB.	-0.277	-0.233	-0.152	-0.216	0.246	-0.113	0.049	0.177
	-0.775	-0.839	-0.794	-0.798	-0.714	-0.635	-0.626	-0.707
MAR.	-0.253	-0.262	-0.254	-0.302	-0.110	-0.201	-0.156	-0.151
	-0.020	-0.057	-0.142	-0.238	-0.274	-0.162	-0.561	-0.541
APR.	-0.094	-0.191	0.091	0.201	0.176	0.301	0.411	0.341
	-0.689	-0.727	-0.697	-0.745	-0.769	-0.716	-0.657	-0.598
MAY	-0.035	-0.031	-0.155	-0.351	-0.428	-0.452	-0.245	-0.272
	-0.359	-0.395	-0.362	-0.297	-0.172	-0.162	-0.145	-0.101
JUNE	-0.126	-0.280	-0.354	-0.315	-0.207	-0.152	-0.061	-0.081
	-0.070	-0.027	0.016	-0.034	-0.132	-0.172	-0.125	-0.053
JULY	0.108	0.044	-0.018	0.018	0.046	0.009	-0.045	-0.027
	0.456	0.350	0.182	-0.005	-0.169	-0.013	0.117	0.041
AUG.	-0.106	-0.184	-0.270	-0.137	-0.004	0.005	0.164	0.172
	-0.101	0.075	0.185	0.123	0.046	0.142	0.210	0.120
SEP.	0.010	-0.084	-0.175	0.005	0.144	0.160	0.111	0.101
	-0.188	-0.274	-0.339	-0.532	-0.567	-0.299	-0.054	0.155
OCT.	-0.415	-0.263	-0.292	-0.233	-0.123	-0.122	-0.113	-0.112
	0.210	0.001	-0.147	-0.256	-0.128	-0.256	-0.123	0.043
NOV.	0.400	0.473	0.512	0.512	0.500	0.496	0.324	0.131
	0.144	0.110	0.069	0.264	0.443	0.105	0.039	0.047
DEC.	-0.070	-0.027	0.016	-0.034	-0.162	-0.171	-0.125	-0.053

JED  
80